TR A7613 - Åpen

Rapport

A study of a Linear Orographic Precipitation Model

Author(s)
Sara Martino
Sjur Kolberg

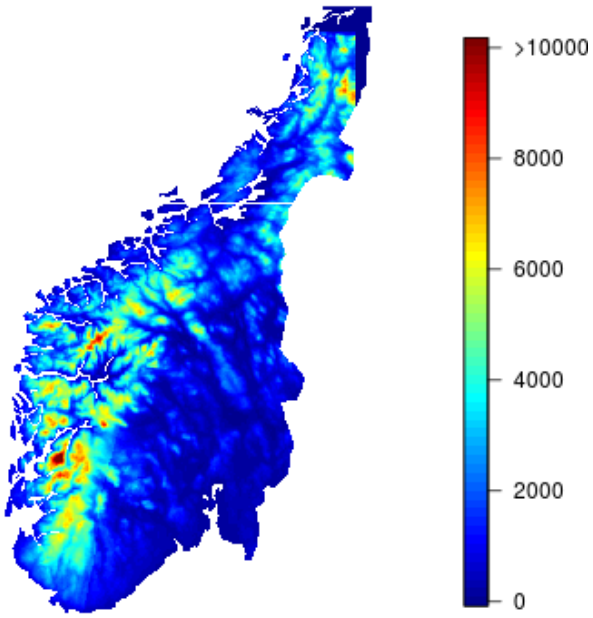

SINTEF Energi AS
Vannressurser
2016-11-30

SINTEF

SINTEF Energi AS
Postadresse:
Postboks 4761 Sluppen
7465 Trondheim
Sentralbord: 73597200

energy.research@sintef.no
www.sintef.no/energi
Foretaksregister:
NO 939 350 675 MVA

Rapport

A study of a Linear Orographic Precipitation Model

VERSJON	DATO
1	2016-11-30

FORFATTER(E)
Sara Martino
Sjur Kolberg

OPPDRAGSGIVER(E)	OPPDRAGSGIVERS REF.
Energi Norge	Oppdragsgivers referanse

PROSJEKTNR	ANTALL SIDER OG VEDLEGG:
502000660	42

Abstract
This report describes the use of a linear orographic model (LOM) to estimate the spatial distribution of precipitation in two case studies. In the first case, the model is driven by spatially homogeneous reanalysis data from the European Centre for Medium range Weather Forecast (ERA-Interim). The simulated values are compared with precipitation observation from a gauge network. Results show that the simulated and observed precipitation are in good agreement for larger accumulation time (months and years). The LOM captures well the main features of climatological precipitation distribution in southern Norway despite the presence of some spatial and temporal biases. For shorter accumulation times, though, the performance is very variable and it was not possible to define stable criteria for discriminating apriori days with good or bad performance. The second case study evaluates LOM as a trend surface generator to support spatial interpolation of precipitation. The forcing data is in this case restricted to surface observations alone. Also, the study area was reduced, and cross validation selected as method, to focus on small-scale covariance. The results showed a slight improvement of the LOM over the traditional lapse rate, but also that the gauge network is too sparse to separate the small-scale performance of the LOM from the nugget effect.

UTARBEIDET AV	SIGNATUR
Sara Martino	Sara Martino
KONTROLLERT AV	**SIGNATUR**
Sjur Kolberg	Sjur Kolberg
GODKJENT AV	**SIGNATUR**
Julie Charmasson	

RAPPORTNR	ISBN	GRADERING	GRADERING DENNE SIDE
TR A7613	978-82-594-3679-5	Åpen	Åpen

A study of a Linear Orographic Precipitation Model

Sara Martino, Sjur Kolberg

December 6, 2016

Contents

1 Introduction **2**

2 Model Description **3**

3 Downscaling Experiment **5**
3.1 Input parameters and model set-up 5
3.1.1 ERA-Interim and Altitude model 6
3.1.2 Moist Brunt-Vaisala frequency 6
3.1.3 Hydrometeor formation and fall-out time 7
3.1.4 Humidity Factor 7
3.1.5 Reduced vapor flux 8
3.1.6 Multi-domain runs 9
3.2 Validation 9
3.2.1 Yearly Precipitation Maps 10
3.2.2 Intermittency Process 12
3.2.3 Precipitation for different accumulation times 20
3.3 Areal accumulated precipitation 25

4 Discussion of the Downscaling Experiment **29**

5 Enki implementation **33**
5.1 Evaluation 34
5.2 Results 35
5.3 Elevation gradient versus Linear Orography Model 35

6 Conclusion and recommendations **39**
6.1 Recommendations 40
6.2 Further work 41

1 Introduction

Spatially distributed precipitation estimates are needed in hydrological modeling and in regional climate analyses. In many areas with complex terrain, like high mountains, regions with glaciers or difficult access, it is challenging to install and maintain a good network of rain gauges. Hence, precipitation maps with high spatial resolution are difficult to obtain. A Linear Orographic Model (LOM) which includes inflow dynamics, condensed water advection, and downslope evaporation was introduced in Smith and Barstad (2004). It is a deterministic method driven by temperature, wind, geopotential and relative humidity. It models the major orographic precipitation processes in a relatively simple and compact formulation, using a small set of equations and a limited number of free parameters.

The LOM is computationally efficient and very fast to run even on a simple desktop; this gives the possibility to produce precipitation fields over large domains at a fine horizontal resolution. In Johannesson (2007) the LOM was used to simulate long time series of precipitation maps over Iceland by downscaling the ERA-40 re-analysis data. The produced data set was compared to precipitation observations from a rain gauge network. The simulated data was found to be, in general, well in agreement with the observed one. This was more true for large accumulation times (month and year) than for daily accumulation.

In the framework of a weather generator, a model like the LOM could serve as a tool to downscale the signal from a numerical weather predictor or a general circulation model, adding details to a relatively smooth map. Precipitation has a complex spatial structure and the LOM considers only one of the physical process connected to precipitation (namely orographic enhancement). Still, the output of the LOM could serve as a "first guess" to which one could add for example a convective precipitation generator.

The first experiment reported in this paper goes in this direction: we use the LOM to downscale the European Centre for Medium range Weather Forecast (ECMWF) re-analysis ERA-Interim and construct daily precipitation maps over the South of Norway with a 1 km horizontal resolution over the period 1990-1999. The produced maps are then compared to precipitation data coming from a gauge net to check the consistency.

Another use of the LOM could be to add terrain-induced variability to the spatial interpolation of observed precipitation data. A well established technique is to use a lapse rate predicting an increase in precipitation with altitude. An orographic justification of this concept is that air being lifted will always increase its relative humidity, hence higher areas have a larger probability of air saturation and precipitation fallout. Once saturated, however, the water release per 100 m continued uplift reduces with elevation. For specific conditions on a given day, the constant lapse rate is therefore an over-simplification.

Replacing absolute altitude with the terrain slope along the current wind vector, as well as using the proper thermodynamic equations for airmass cooling and condensation, is the basis for the 'raw upslope model' Smith and Barstad (2004). The LOM is a further elaboration of this idea, taking into account also air mass dynamics, atmospheric stability and the time scale of hydrometeor formation and fallout. The LOM can therefore be

regarded as a more physically plausible alternative to the fixed precipitation lapse rate used in precipitation interpolation. The second experiment in this report investigates this idea in a relatively small area in central Norway.

In what follows, a brief model description is given in Section 2. The downscaling experiment is described in Section 3. The input and the model parametrization are described in Section 3.1. Section 3.2 describes the results of the validation, considering various temporal scales and statistical characteristics. Section 4 is a discussion of the first experiment. Section 5 describes the second experiment and the ENKI implementation of the LOM. Finally, section 6 concludes the report.

2 Model Description

In this section we provide a brief description of the LOM. Most of this section is taken from Smith and Barstad (2004) and Johannesson (2012).

The Linear Orographic Model (LOM) proposed by Smith and Barstad (2004) simulates precipitation over complex terrain. First, assuming that air is saturated or near saturation and flows over the terrain (no flow splitting and no stagnation), the distributed source of condensed water, $S(x, y)$, resulting from terrain-forced vertical ascent of moist air is calculated as follows:

$$S(x, y) = \frac{C_w}{H_w} \int_0^\infty w(x, y, z) e^{-z/Hw} \, dz \tag{1}$$

The vertical velocity, $w(x, y, z)$, is assumed to vary with altitude. At ground level, $w(x, y, z = 0) = U \cdot \nabla h(x, y)$, where U is the horizontal wind-speed vector and $\nabla h(x; y)$ the topographic gradient. H_w is the depth of the moist layer (or water vapor scale height):

$$H_w = -\frac{RT_{ref}^2}{L\gamma} \tag{2}$$

$R = 461 JkgK^{-1}$ is the gas constant for water vapor, $L = 2.5 \cdot 10^6 Jkg^{-1}$ is the latent heat and T_{ref} is the temperature at the ground. The term

$$C_w = \frac{\rho_{s_{ref}} \Gamma_m}{\gamma}$$

is the thermodynamics uplift sensitivity factor relating condensation rate to vertical motion. Γ_m is the moist adiabatic lapse rate. The term

$$\rho_{s_{ref}} = \frac{e_s(T_{ref})}{RT_{ref}}$$

is the saturation water vapor density and e_S is the saturation vapor pressure. The advection of condensed water by the mean wind and the resulting precipitation is described by the following equations:

$$\frac{Dq_c}{Dt} \approx U \cdot \nabla q_c = S(x, y) - \frac{q_c}{\tau_c} \tag{3}$$

$$\frac{Dq_s}{Dt} \approx U\nabla q_s = \frac{q_c}{t_c} - \frac{q_s}{\tau_f} \tag{4}$$

Where $q_c(x, y)$ represents the vertically integrated cloud water density, $q_s(x, y)$ represents the vertically integrated hydro-meteor density, t_c is the conversion time from cloud water into hydro-meteors, t_f is the hydro-meteor fallout time and q_s/τ_f represents the precipitation rate.

The solution of Eqs. (3) and (4) is obtained by taking the Fourier transforms of Eqs. (1), (3) and (4). The dynamics of the forced ascent, $w(x, y, z)$, is described using results from mountain wave theory, which in Fourier space leads to $\hat{w}(k, l, z) = \hat{w}(k, l, 0)e^{imz}$, with $\hat{w}(k, l, 0) = i\sigma\hat{h}(k, l)$. The term $s = U_x k + U_y l$ is the intrinsic frequency which defines the wind vector in Fourier space, k and l the horizontal wave numbers, $m = [(N_m^2 - \sigma^2)\sigma^{-2}(k^2 + l^2)]^{1/2}$ the vertical wave number and N_m the moist Brunt-Vaisala frequency.

After some algebra, the double Fourier transform of the precipitation field is given by the following transfer function:

$$\hat{P}(k, l) = \frac{C_w i\sigma\hat{h}(k, l)}{(1 - imH_w)(1 + i\sigma\tau_c)(1 + i\sigma\tau_f)} \tag{5}$$

where the double Fourier transform of the terrain is given by

$$\hat{h}(k, l) = (2\pi)^{-2} \int\int h(x, y)e^{-i(kx+ly)}\, dxdy \tag{6}$$

Eq.(5) states that the spatial relocation of precipitation by topographic uplift is controlled by several partly counteracting processes, namely airflow dynamics, cloud time scales, and the advection of condensed water and hydrometeors. The amount of water vapor that can be condensed (the source term $S(x, y)$) depends on the moist layer depth and the ability of the forced vertical ascent to penetrate through this moist layer, which is controlled by airflow dynamics. The condensation is reduced if the vertical uplift does not penetrate through the moist layer. Also, an increase of stability (N_m) will cause the available water vapor to increase (C_w and H_w) but will reduce the depth of the lifting (increasing m).

If t_c is short, condensed water will be formed quickly on the windward side and start to precipitate before being advected downstream to the lee-side of the mountain where it evaporates. If t_f is short, precipitation will mainly fall on the windward side of the mountain while if it is long, spill-over will take place and precipitation will also fall on the lee-side. This also means that for given t_c and t_f values, the resulting precipitation pattern will depend on the width of the mountain and the wind speed. High wind speeds may advect air parcels over the lee-side before water vapor has time to condense and fall. Large values of t_c and t_f will shift the condensation and precipitation downstream. The residence time of an air-parcel on the windward side of a large mountain will be longer than on a smaller one, increasing the amount of water that can be condensed and precipitation that can be formed. A detailed description of changes in spatial precipitation

patterns and location of maximum precipitation in response to changing atmospheric conditions, mountain geometry and horizontal topographic scales can be found in Smith and Barstad (2004) and Barstad and Smith (2005).

The precipitation field is finally retrieved by taking the inverse Fourier transform of Eq. (5) and truncating negative values of the total precipitation:

$$P(x,y) = \text{Max}\left[(\int_{-\infty}^{\infty}\int_{-\infty}^{\infty} \hat{h}(k,l)e^{i(kx+ly)}\ dk\ dl + P_\infty), 0 \right] \tag{7}$$

The term P_∞ indicates the background precipitation or non-orographic precipitation.

A practical advantage of the LOM is its ability to encapsulate the major processes governing orographic generation of precipitation in a simple and compact formulation. The limited input parameters, namely P_∞, U, V, T, N_m, τ_c and τ_f, make it fast to implement and run even with high spatial resolutions and long time periods.

The main model limitations are the simplification of the vertical structure of the atmosphere and the assumption of a horizontal uniform background flow and atmospheric properties. Moreover, non linear effect such as flow blocking are not captured and the model does not work for unstable atmosphere. Finally the atmosphere is assumed to be saturated.

The assumption of horizontal uniform background atmospheric conditions means that temperature wind vectors, static stability and cloud delay times are assumed constant in space.

The assumption of saturated atmosphere implies that time and/or space windows defining when and where the model can be applied have to be defined. This will be discussed further on.

Finally the assumption of constant vapor flux, together with the model assumption that precipitation is proportional to vapor flux means that the air mass is not depleted of its humidity downwind. A post-processing algorithm aiming at (partially) fixing this will be discussed later.

3 Downscaling Experiment

In this section we describe the first experiment with the LOM. The goal is to use the LOM to create time series of precipitation maps over the south of Norway and then compare the simulated data set with precipitation data coming from a grid of 197 rain gauges belonging to the Norwegian Meteorological Institute (MET). The spatial distribution of the rain gauges is represented in Figure 1b)

3.1 Input parameters and model set-up

The input parameters needed by the LOM can either be derived directly from re-analysis data set such as ERA-Interim or considered as free parameters whose value can be optimized to better fit observed data. In this report, following Johannesson (2012), we have tried to link as many of such parameters as possible to physical measurements.

We describe here the input parameters, the model set up and some post-processing algorithms aimed at correcting some of the known limitation of the LOM.

3.1.1 ERA-Interim and Altitude model

The input meteorological data to the LOM have been derived from the ECMWF re-analysis (ERA-Interim). The time step of the ERA-Interim re-analysis is 6 hours, that is 4 data points for each day.

The input meteorological data include:

- Geopotential height at two different pressure levels (850 and 1000 hPa)
- Temperature at two different pressure levels (850 and 1000 hPa)
- Wind vector at 850 hPa
- Relative humidity at 850 hPa
- Total precipitation

The choice of the pressure level from which to extract the input meteorological variables was done following Crochet (2007).

With the exception of the relative humidity, all meteorological data where averaged over the whole geographical area of interest. The relative humidity was used as a "soft" threshold to determine the areas with precipitation, see Section 3.1.4.

In Johannesson (2012) the whole spatial information about background precipitation contained in the ERA40 re-analysis was fully exploited. In this report we instead retain only the spatial average.

The orographic model is defined over a 1×1 km grid, see Figure 1a)

3.1.2 Moist Brunt-Vaisala frequency

In Crochet (2007) the value of the Moist Brunt-Vaisala frequency (N_m) was optimized and then assumed to be constant over the whole time period. We follow Johannesson (2012) and estimate N_m at each time step according to the atmospheric conditions.

The Moist Brunt-Vaisala frequency (N_m) was estimated after Smith and Barstad (2004) as

$$N_m = \frac{g}{T}(\gamma - \Gamma_m)$$

where g is the gravitational acceleration constant. γ is the environmental lapse rate computed as $(z_A - z_B)/g$ where z_A and z_B are the geopotential height at two different altitudes. Γ_m is the moist lapse rate computed as $0.1T_{ref} - 34.3$ (Celsius/Km) as in Smith and Barstad (2004).

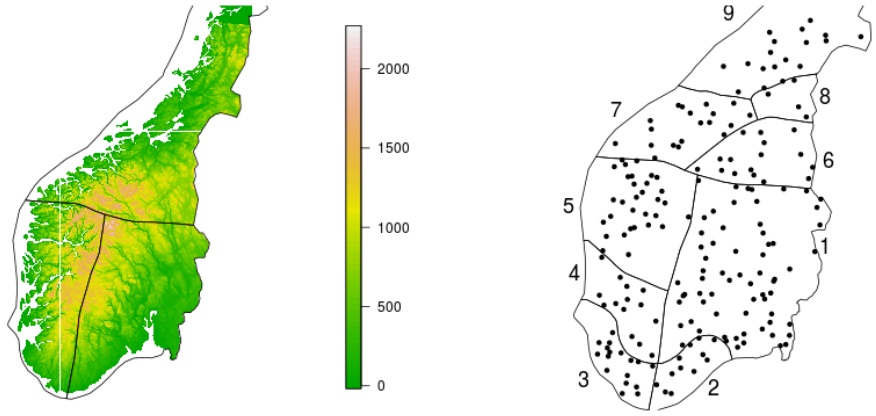

a) b)

Figure 1: a) Altitude Model with location with superimposed the three regions used to compute the input parameters for the LOM. b) Location of the 197 gauge stations used for validation. Superimposed are the limits of the 9 areas used for validation purposes.

3.1.3 Hydrometeor formation and fall-out time

The parameters τ_c and τ_f express the time it takes for hydrometeors to form after condensation, and to fall to the ground, respectively.

The hydrometeor formation time τ_c was considered constant in time and fixed to 1800 seconds. This value was chosen after optimizing some preliminary runs of the LOM.

The fall-out time τ_f was defined as in Johannesson (2012):

$$\tau_f = H_w/V_t \text{ with } \begin{cases} V_t = 1\ m/s, & \text{if snow} \\ V_t = 6\ m/s, & \text{if rain} \end{cases}$$

where H_w is the water vapor scale height, and V_t is the fall velocity, with approximate values for snow and rain, respectively.

3.1.4 Humidity Factor

As stated earlier, the LOM assumes saturated atmosphere. It is therefore necessary to establish a criterion which indicates in which time steps or in which part of the domain the LOM can be run.

In a first attempt to run the LOM we used the spatially averaged relative humidity as a threshold, set to 80% at 850 hPa, to define when the model could be run. This meant that, when the mean humidity was below threshold the model could not be run and we assumed that all the stations in the domain were dry. On the other side, when

the mean humidity was above the threshold, the LOM was run with the assumption that the atmosphere was saturated over the whole domain. This lead, on one side, to too many time steps when the domain was completely dry, and, on the other side, to a too strong spatial correlation for the time steps for which the model was run.

In both Johannesson (2007) and Crochet (2007), the use of the LOM was restricted within pre-existing wet areas defined by the background precipitation fields in the ERA Interim dataset, and a constant humidity threshold so as to guarantee that near saturated conditions were met.

In this report, we choose the approach of Johannesson (2012) where, as suggested also in Sinclair (1994), a local humidity factor was introduced to better define the limits of application of the model and reduce precipitation when unsaturated conditions prevail. In Sinclair (1994), this humidity factor is defined as

$$\lambda(x,y) = \begin{cases} \left(\frac{RH_{x,y}-RH_{min}}{\beta}\right)^{\delta} & \text{if } RH_{x,y} < RH_{min} \\ 0 & \text{otherwise} \end{cases}$$

where $RH_{x,y}$ is the low-level relative humidity taken at 850 hPa, $RH_{min} = 80\%$ is the lower relative humidity threshold below which no orographic precipitation is formed. β and δ are adjustable parameters taken as $\beta = 20$ and $\delta = 0.3$.

The precipitation field from the LOM is then corrected as follows:

$$P_{corr}(x,y) = P(x,y)\ \lambda(x,y) \tag{8}$$

To compute the humidity factor $\lambda(x,y)$ the low level humidity field $RH_{x,y}$ was estimated at each grid point by bi-linear interpolation from the corresponding relative humidity field in the ERA-Interim data set.

3.1.5 Reduced vapor flux

In the original formulation (Smith and Barstad, 2004), the LOM expresses precipitation as proportional to the upstream water vapor flux, which is held constant over the whole domain of interest. This means that for two hills with the same orographic structure the LOM will simulate the same amount of precipitation, even if the second hill is located in the rain shadow of the first one.

In a real case of a domain with a succession of mountain ridges, precipitation causes the water vapor flux to be depleted downwind as the airflow passes over several hills and orographic precipitation is formed, so that downwind located hills will receive less or no precipitation.

In order to deal with this, Smith and Evans (2007) made the assumption that precipitation is proportional to the local water vapor flux and proposed to scale the precipitation down with the local fraction of water vapor remaining, as follows:

$$P_{reduced}(x,y) = P(x,y)\Theta(x,y) \tag{9}$$

where $P(x, y)$ is computed with Eq. (7) and $\Theta(x, y)$ is the fraction of vapor remaining defined as

$$\Theta(x, y) = 1 - \int_{-\infty}^{x,y} P_{reduced}(x', y') ds / F_0$$

where $F_0 = \rho q_w U H_w$ is the incoming upstream horizontal water vapor flux and $ds = (U_x dx' + U_y dy')/|U|$. After some manipulations this leads to:

$$\Theta(x, y) = e^{DR_{ref}(x,y)};$$

where

$$DR_{ref}(x, y) = \int_{-\infty}^{x,y} P(x', y') \; ds / F_0 :$$

In our case, $P(x, y)$ is replaced by $P_{corr}(x, y)$ in and the final precipitation estimate is given as

$$P_{reduced}(x, y) = P_{corr}(x, y)\Theta(xy) \tag{10}$$

In practice, each precipitation map is produced as follows:

1. Compute $P(x, y)$ from Equation 7
2. Correct for the humidity factor as in Equation 8, and obtain $P_{corr}(x, y)$
3. Correct for the reduced vapor flux as in Equation 10 and obtain the final precipitation field $P_{reduced}(x, y)$

The four maps related to the same day are then added to each other in order to form a daily precipitation map.

3.1.6 Multi-domain runs

For each model set-up, the model was run three times per time step over the entire domain so as to better represent the spatial variability of atmospheric conditions, especially the mean wind whose direction may vary within the domain and will have a strong impact on the spatial pattern of precipitation. In practice, the input meteorological parameters (except the humidity field) where calculated for three different sub-domains and the LOM applied each time to the entire domain but the resulting precipitation corresponding to each sub-domain only was selected. The final precipitation map was obtained by merging the precipitation by each sub-domain. These domains roughly correspond to homogeneous climatic zones (see Figure 1a).

3.2 Validation

The goal of our validation exercise is to understand weather the LOM can reproduce some of the statistical characteristics of precipitation over the South of Norway. To do so we produce daily precipitation maps using the LOM for the period 1990-1999, select the time series relative to the spatial locations where the observation stations lies and compare such simulated time series of precipitation with the observed ones.

We want to establish how well the simulated data set can reproduce the occurrence process (that is if it raining or not) of the precipitation over the South of Norway We are interested in comparing observed and simulated precipitation at different time scales: daily, monthly and yearly. Moreover, it is of interest to validate both the at-site distribution and some regional summaries statistics that involve also the correlation structure of the data set.

It is important to keep in mind that no precipitation data from gauges is used in running the LOM and the only information about precipitation coming from ERA-Interim is a spatially averaged value of total precipitation. Moreover, all input parameters, except for the humidity field, are averaged over the domain of interest.

3.2.1 Yearly Precipitation Maps

Before presenting the quantitative results, it is useful to provide a qualitative evaluation of the maps produced by the LOM. Figure 2, panels a) and b) show maps of the annual precipitation for two of the ten years considered in this study, 1990 and 1992. The maps are built as spatial mosaics from the maps for each of the three sub-domains. No effort was made to smooth the transition from one sub-domain to the other. Such transition is especially visible for the 1990 map.

As comparison, Figure 2, panels c) and d), display also maps of annual precipitation created by MET. These maps based on the precipitation data collected by the rain gauge network and computed using a smoothing algorithm. The two set of maps (LOM and MET maps) are produced in very different ways and should not be expected to produce the same result when compared pixel by pixel. Still, is is fruitful to check how closely the spatial distribution of precipitation as simulated by the LOM resembles the smooth interpolated map.

There are some significant differences between the two sets of maps, the largest ones are in the degree of resolution, the amount and the spatial distribution of precipitation. The maps produces by LOM are much more detailed than those from MET. This is as expected, given that the LOM simulates processes operating at smaller scales than the gauge network represents, whereas the interpolation has a strong smoothing effect. Further, the LOM appears to overestimate the yearly precipitation especially in some areas of the west coast. The areas with large annual precipitation, in the MET maps limited to the west coast, extend in the LOM maps eastwards towards the main water divide, but not as a continuous surface. This could be a sign that the post-processing algorithm described in Section 3.1.5 does not deplete the water vapor flux sufficiently, causing precipitation events coming from the ocean to penetrate too much inland.

Finally, it is worth noting that the strongest differences between the LOM and MET maps of annual precipitation, occur in mountainous areas poorly covered by the gauge network. The main mountain range and some of the main glaciers to the west of this stand out as large-precipitation areas, which appears plausible, but non-verified due to the lack of data.

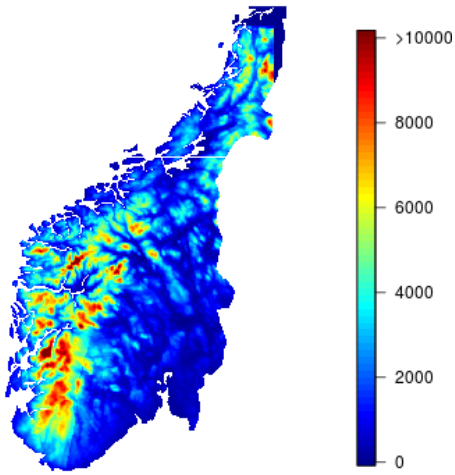

a) 1990 LOM map

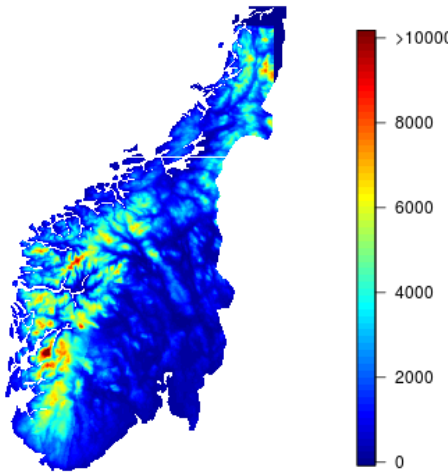

b) 1992 LOM map

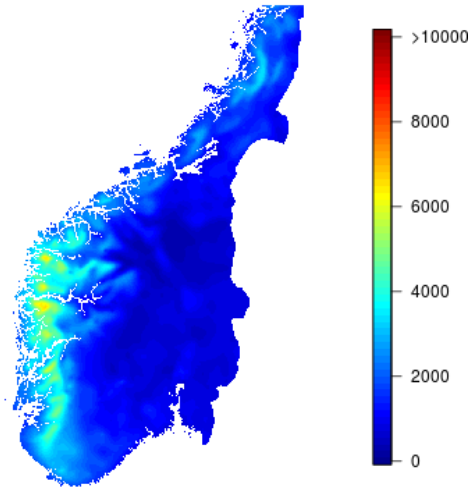

c) 1990 MET map

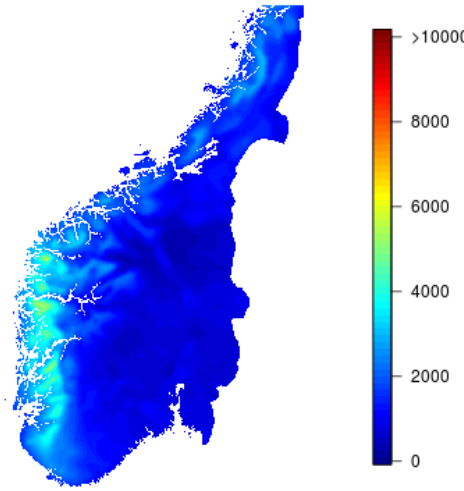

d) 1992 MET map

Figure 2: Yearly Precipitation maps produced by the LOM, panels a) and b) and smoothed yearly precipitation maps from MET, panels c) and d).

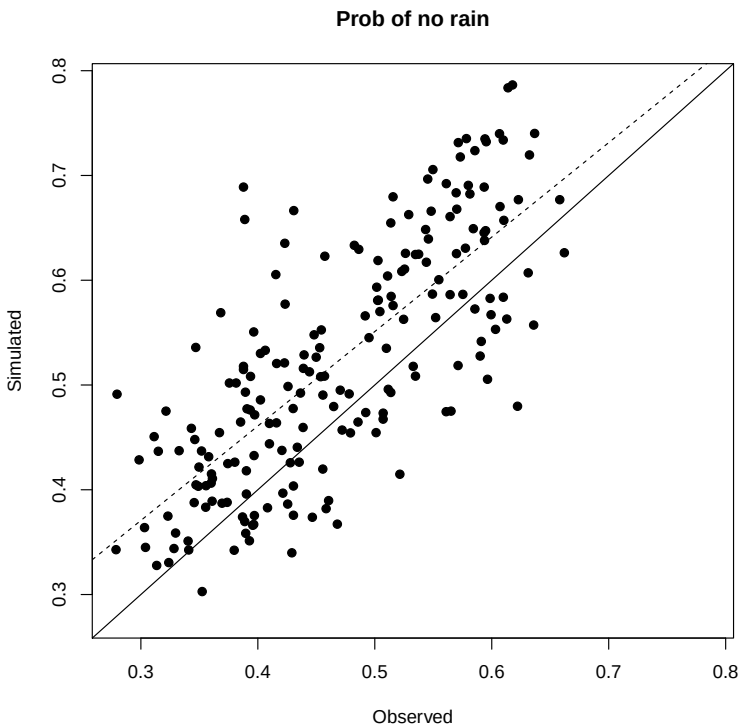

Figure 3: Observed and Simulated Probability of no-rain P_0 for all the stations. The solid and dashed lines represent the 1:1 relation and the best-fit regression line, respectively. The value of R^2 is 0.56.

3.2.2 Intermittency Process

In this section we discuss how well the LOM describes the intermittency process of precipitation, that is, the spatio-temporal pattern of rain vs no-rain.

Figure 3 shows the observed and simulated probability of daily no-rain, p_0, for the different stations. The spatial variability is well represented. The coefficient of determination R^2 between observed and simulated p_0 is 0.56. There is a moderate positive bias in the predictions, so p_0 is more often overestimated than underestimated. Figure 4 reveals that such overestimation has a clear spatial pattern. While the correspondence is very good along the coastline, the LOM clearly overestimates the probability of dry state in the interior of the country.

When computing the daily probability of no-rain disaggregated at a seasonal level, we notice also a seasonal pattern in the agreement/disagreement of observed and simulated data set. Figure 5 shows that the largest biases in the estimated seasonal daily probability of no-rain happen in the summer period ($R^2 = 0.34$). Some of the stations, mainly located again in the interior of the country, see Figure 6, have a simulated probability of being dry close to 90% while the observed one is just above 50%. Given the

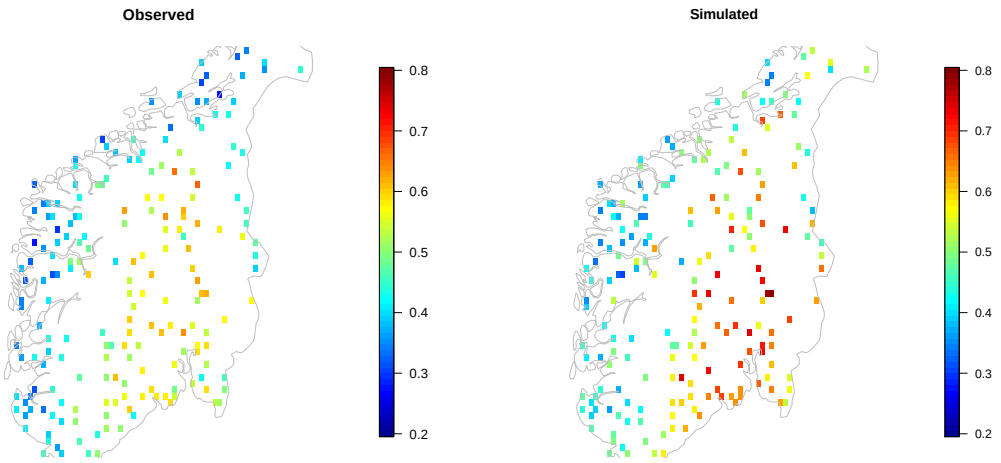

a) b)

Figure 4: Spatial distribution of P_0 for the observed a) and simulated b) data set.

nature of the LOM, which is meant to model orographic precipitation, such results are not too surprising. In particular away from the coast and during summer, convection is an important process causing precipitation, but not represented in the LOM.

One important characteristic of the intermittency process is the at-site probability of transition between dry and wet state. Such probabilities describe, for example, how probable it is that a wet day is followed by a dry one. We define the quantity:

$$p_{ij} = \text{Prob}[\text{state } j \text{ on day } t | \text{state } i \text{ on day } t-1] \; i, j = 0, 1$$

where $i = 0$ indicates dry state and $i = 1$ indicates wet state.

The LOM itself does not explicitly simulate the time dependence between precipitation in different time steps; this information arises only from serial dependency in the input forcing from ERA Interim. In other words, LOM works independently with each time step. Still, by modulating the input signal differently for each location according to time varying input, the LOM introduces spatial variability in the temporal interdependencies, and transfer temporal interdependencies between variables. Hence, it is meaningful to assess the temporal dynamics of LOM output as property of the LOM; different from, but not independent of the temporal dynamics of its input.

As it turns out, LOM reconstructs the transition probabilities with considerable skill for all the stations in the domain, including their spatial variability (Figure 7). As expected, the probability of rain given that the previous day was wet p_{11}, is higher (almost double) than the same probability given that the previous day was dry p_{01}, and this is well captured by the LOM. For the stations in the interior of the country (plot not reported here) the simulated values of p_{00} are too high (and p_{01} are too low). This

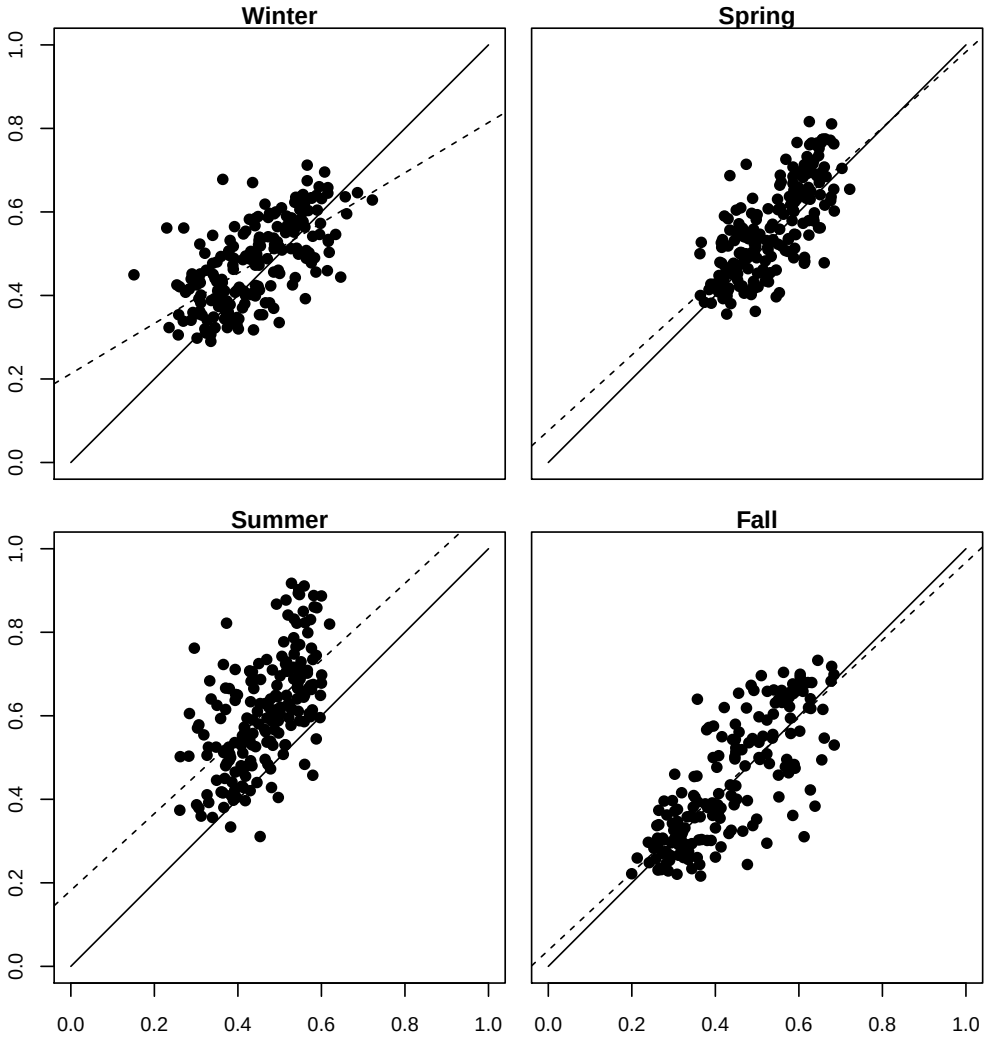

Figure 5: Observed (x-axis) and Simulated (y-axis) probability of no-rain P_0 in the four season of the year. The solid (dashed) lines are the 1:1 (regression) lines. The R^2 values are (0.42,0.52,0.34,0.62) for (Winter, Spring, Summer, Winter)

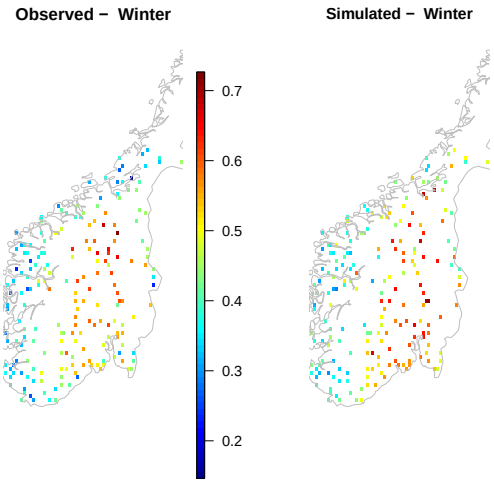

a) Winter

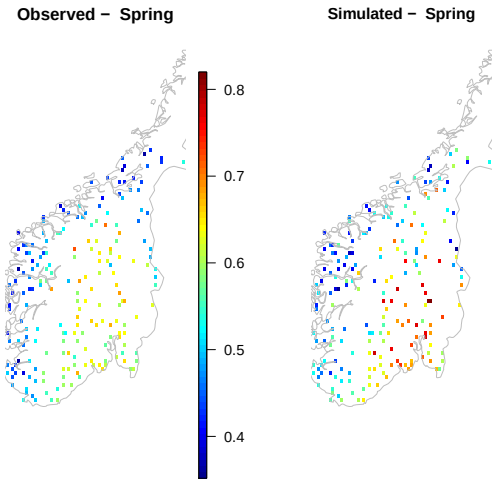

b) Spring

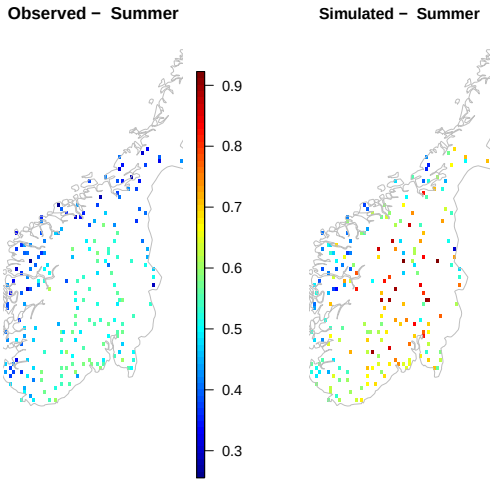

c) Summer

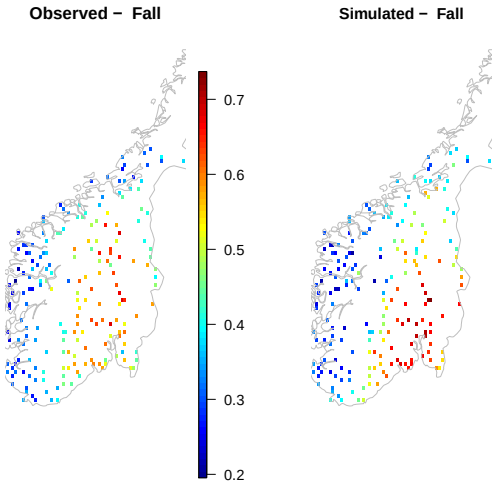

d) Fall

Figure 6: Spatial distribution of seasonal P_0 for the observed (left) and simulated (right) data set.

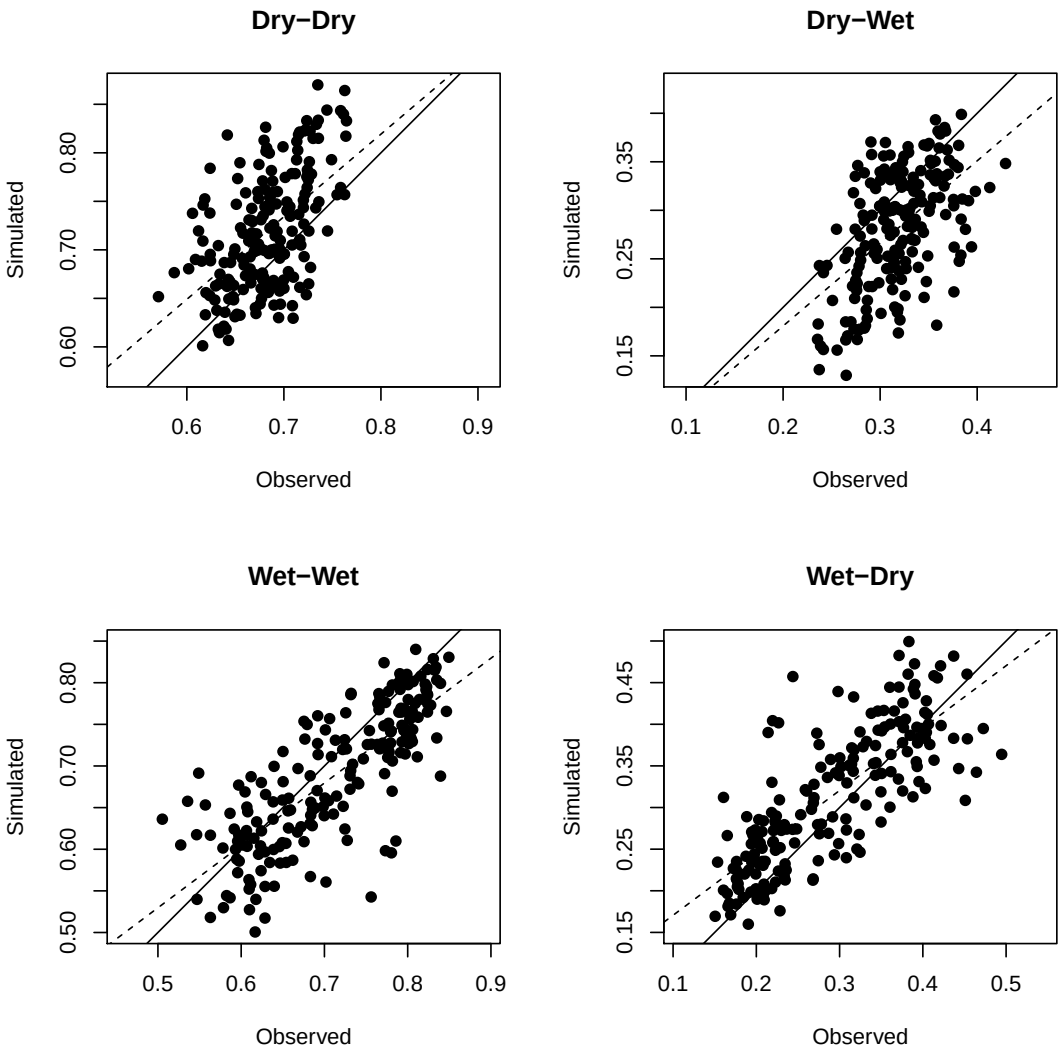

Figure 7: Observed and simulated probability of transition from dry to dry state p_{00}, dry to wet state p_{01}, wet to dry state p_{10} and wet to wet state p_{11} computed over the four seasons. The solid (dashed) lines are regression (1:1) lines.

means that, according to the LOM, for the stations in the interior of the country it is more probable to be dry and to stay in the dry state than it is observed through the data. The remaining two probabilities p_{11} and p_{10} are better represented by the LOM.

One important feature of the precipitation phenomenon, which is also difficult to reproduce, is the length of wet and dry spells, that is the number of days during which one stations stays in the wet or in the dry state. We have computed the mean and the standard deviation of the length of dry and wet spell periods for both the observed and the simulated data set. Figure 8 shows these quantity plotted against each other. While the LOM seems to reproduce the mean and sd of the wet spells quite well ($R^2 = (0.64, 0.56)$ respectively), the length of dry spells is worse explained. The R^2 index is 0.35 for the mean and 0.34 for the standard deviation. Moreover, the length of dry spell is largely overestimated for many stations inland (Fig 9). This is, of course, in agreement with the fact that for the same stations the probability of staying dry is overestimated while the probability of transition from dry to wet state is underestimated (Figure 7).

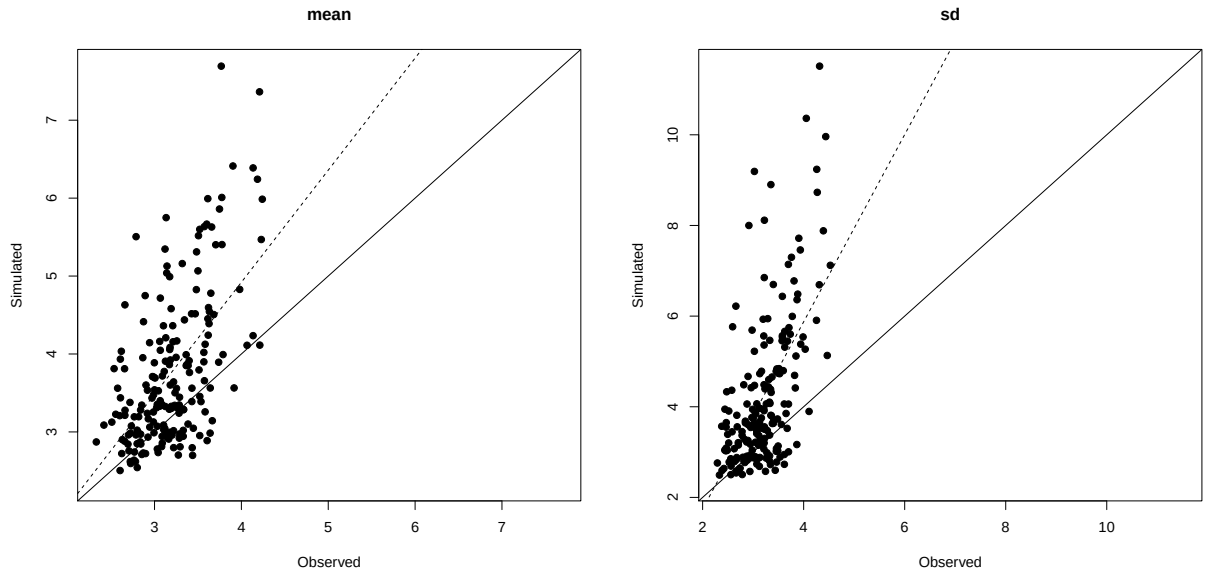

a) Mean dryspell length

b) Sd of dryspell length

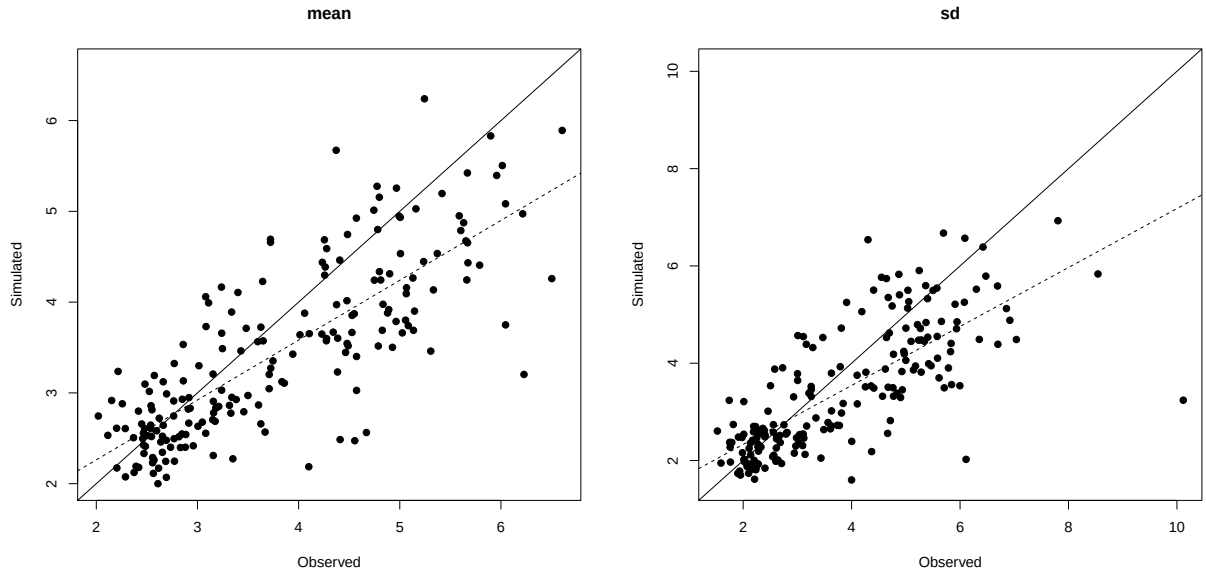

c) Mean wetspell length

d) Sd of wetspell length

Figure 8: Observed vs simulated mean and sd of the length of dry and wet spell periods for all the stations. Solid lines represent the 1:1 relation and dashed lines the best-fit linear regression model.

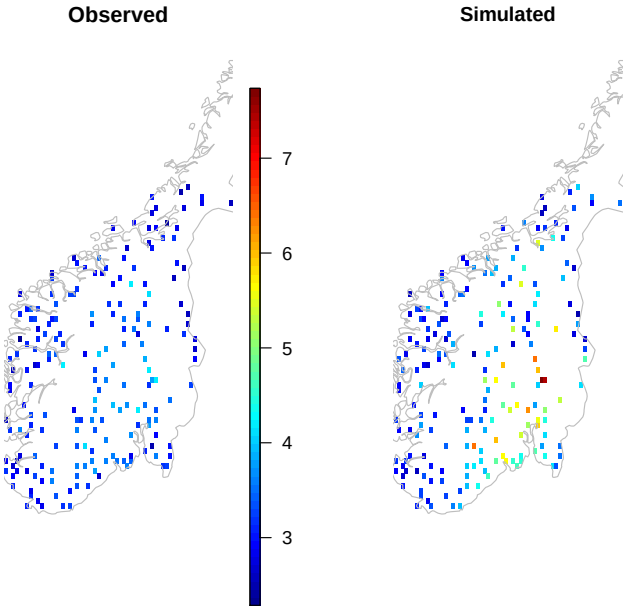

Figure 9: Spatial distribution of the mean length of dry spell period for observed (left) and simulated (right) data set.

	Daily	Weekly	Monthly	Yearly
LOM	0.40	0.65	0.67	0.73
ERA-Interim	0.49	0.73	0.75	0.73

Table 1: Linear correlation between observed and simulated precipitation over different accumulation periods for the LOM simulated data set and the ERA-Interim data

3.2.3 Precipitation for different accumulation times

We want to compare the simulated and the observed data set over different accumulation times. Figure 10 displays observed vs simulated precipitation amounts at daily, weekly, monthly and yearly accumulation. The monthly (weekly) accumulations are computed for each month (week) of each year. The LOM performance improves considerably with the accumulation period, as shown in Table 1 where the linear correlations between observed and simulated data are reported. The same table reports also the correlation coefficients computed by comparing observed data and precipitation extracted directly from the ERA-Interim data base. ERA-Interim performs better especially at the lower accumulation time, it is equivalent to LOM for the yearly accumulation. When comparing the scores of ERA-Interim and LOM it has to be kept in mind LOM achieves this skill level for detailed, information-rich precipitation maps, whereas the ERA-Interim predictions are smooth surfaces for which locational errors produce only small residuals. Still it is clear, at small accumulation times ERA captures some processes that are not captured by LOM. We believe that one of the problem of the LOM is its difficulty, with the parametrization taht we used, to well identify, especially in some days, the wet and dry areas, see all the discussion below about days with bad and good performance

At the daily scale the correlation is quite low. When we compute correlation for each station separately (Fig 11) we notice two things:

- The correlation values have a quite large spatial variation
- There is a clear spatial structure, with the stations along the coast being much better simulated than those inland.

If we look at the daily performance of the LOM, comparing observed and simulated precipitation day by day, we observe that the model performed well in many cases but in others (not a negligible number) the performance was quite poor. An inspection of a high number of cases indicated that a very large source of discrepancy was a wrong identification of the wet and dry regions, leading sometimes to very large errors. Maybe using the whole total precipitation field from ERA-Interim and not just the spatial mean as background precipitation in equation 7 would help improving this. Still Johannesson (2012), who did not average the total precipitation field, noticed the same kind of problem in their experiment.

Some effort was made to try to identify characteristics of the input variables which lead to good or poor simulations. For example, we made the hypothesis that in days with less stable atmosphere the simulations would be bad, or that the performance of

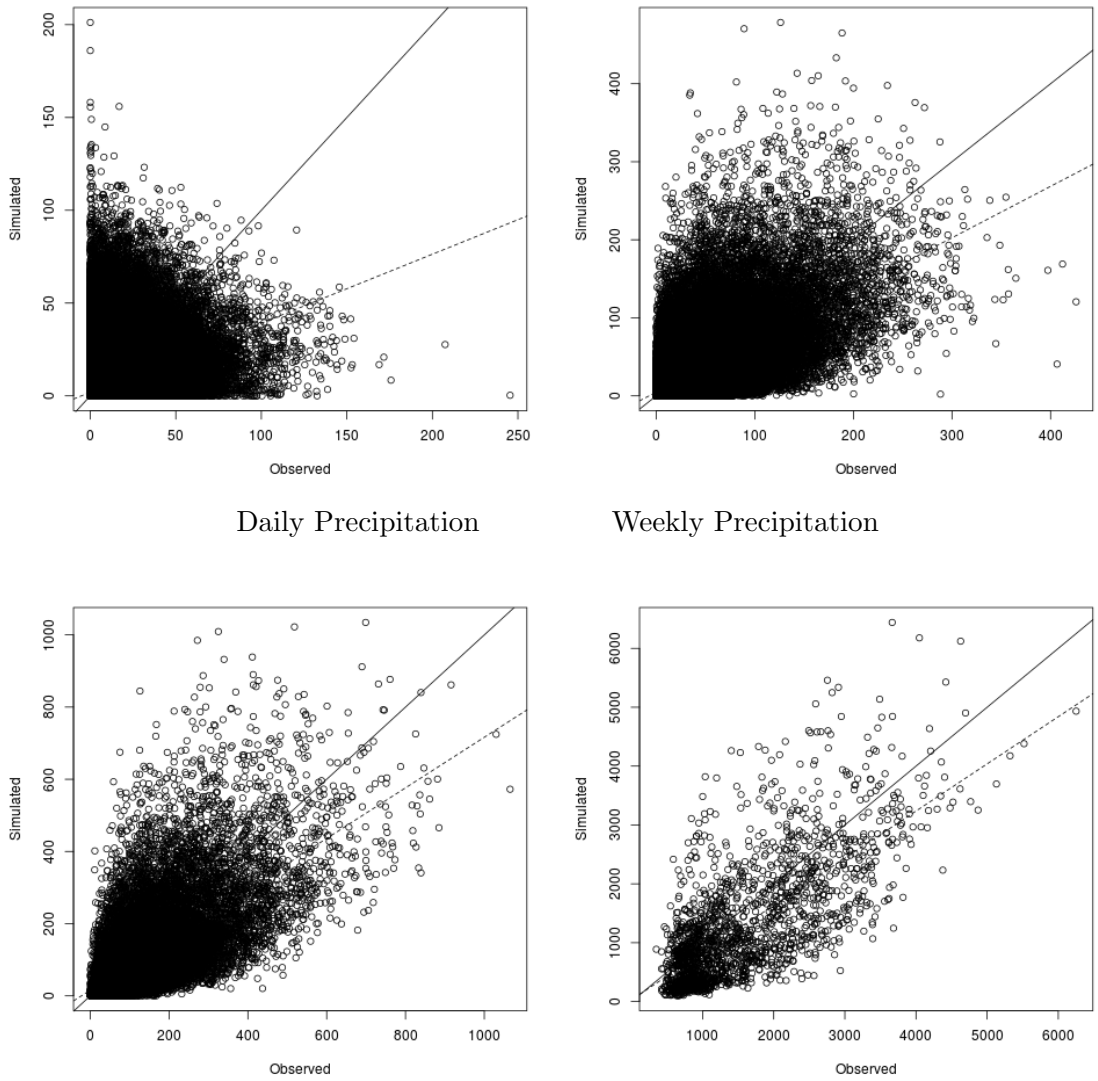

Daily Precipitation Weekly Precipitation

Monthly Precipitation Yearly Precipitation

Figure 10: Observed vs simulated precipitation at different accumulation times. Daily (upper left), weekly (upper right), monthly (lower left) and yearly (lower right). The solid (dashed) lines are regression (1:1) lines.

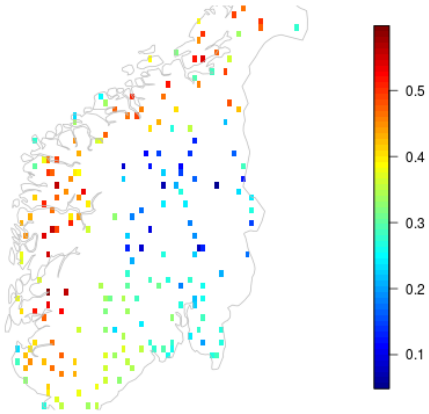

Figure 11: Correlation index between observed and simulated precipitation for each stations.

simulations was linked to the wind direction of strength. These and a variety of other relationships were evaluated, but unfortunately we did not manage to find a reliable criterion to discriminate apriori in which conditions the LOM performs well or poorly. To illustrate what to expect from the model performance when run on a day-to-day basis, we presents a validation for two days (September 16th 1997 and December 4th 1998) when the LOM performed very good and very bad, respectively.

Figure 12 illustrates the situation on a day when the LOM manages to replicate the observed precipitation pattern well. Panel d) in Figure 12 shows the wind direction in the tree sub-regions for the four time points belonging to the day in discussion. The westerly wind brings quite a lot of precipitation on the west coast and no precipitation on the east side of the mountains. The LOM correctly identifies the wet and dry areas, and manages to replicate, more or less correctly, also the amounts of precipitation. Panel e) in the same figure is the precipitation map extracted from ERA Interim, the detail level is quite low but clearly the wet area is the same as in the observed data set and in the LOM simulations.

Figure 13 illustrates the situation on a day when the LOM performance is poor, in this case because the large-scale location of the wet and dry areas is wrong. Panel d) in Figure 13 shows that the wind blows from the east-northeast, and this signal is quite homogeneous in both space and time. Still rain is only observed on the west coast. The LOM simulates rain on the east side of the mountains thus showing a precipitation pattern totally different from the observed one. The ERA Interim map in panel e) displays the correct location of the wet area at the northwestern coast (in addition to a strong event over western Sweden, not detected by the Norwegian gauge network). The humidity map used as a threshold to identify areas with high humidity as explained in

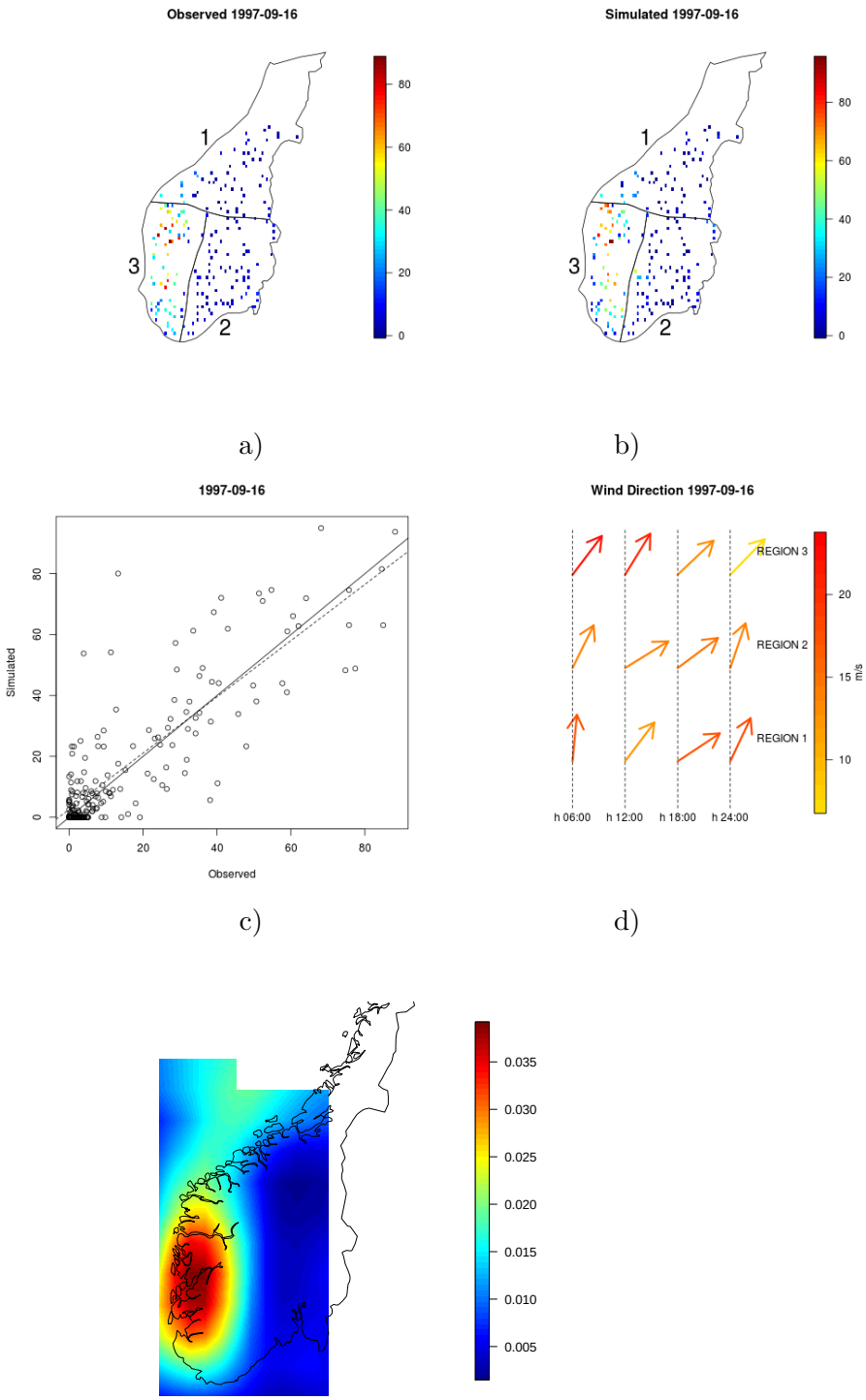

Figure 12: Precipitation on 1997-09-16, observed a) and simulated b). Panel c) plots observed and simulated precipitation against each other. The solid (dashed) lines are 1:1 (regression) lines. Panel d) shows the input wind vector for the 3 sub-domains and the 4 time points. Panel e) displays a precipitation map from ERA Interim.

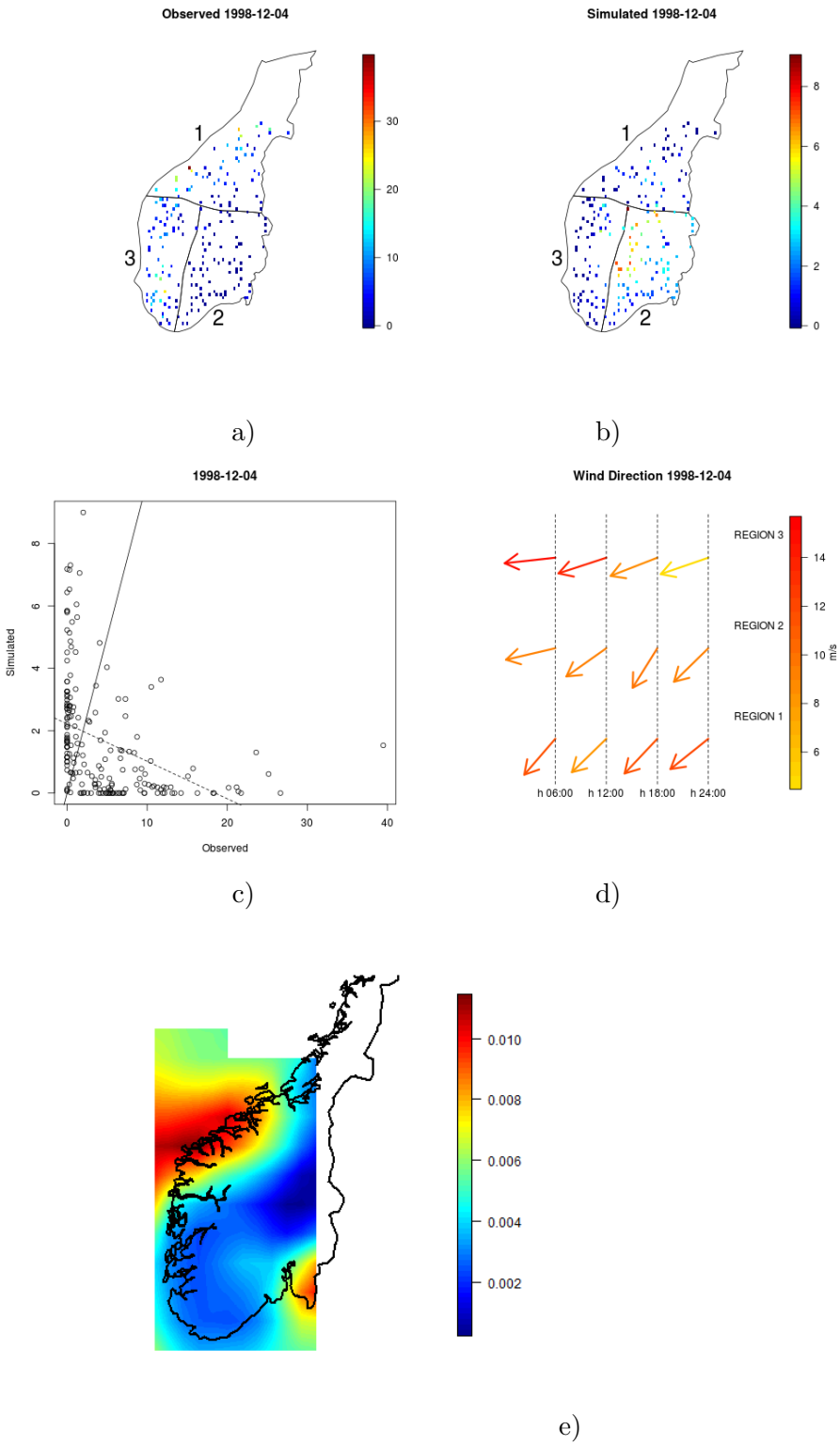

Figure 13: Precipitation on 1998-12-04, observed a) and simulated b). Panel c) plots observed and simulated precipitation against each other. The solid (dashed) lines are 1:1 (regression) lines. Panel d) shows the input wind vector for the 3 sub-domains and the 4 time points. Panel e) displays a precipitation map from ERA Interim.

section 3.1.4 does not help in this case to identify the wet areas as it is quite homogeneous and above 80% for the whole south of Norway (not shown).

These two days were chosen randomly between those with good and bad performance but they illustrate the difficulty of finding criteria which indicate apriori when the LOM is going to perform well.

Some statistical characteristics of the daily precipitation were estimated each year and for each month over the period 1990-1999 at each of the 197 stations. We computed the mean and some quantiles (25%, 50%, 75% and 90%) for precipitation larger than 0.1 mm plus the probability of no-rain. These quantities are illustrated in Figure 14. The global performance is not impressive but the performance for region along the coast is considerably better, also the summer months are particularly bad represented, as noticed also earlier (not shown). The probability of no-rain also appears quite poorly estimated, with the same time and space variability in performance as for the other statistical quantities.

At the monthly scale the LOM appears to be able to capture the main characteristics of the precipitation process but presents some temporal biases. Figure 15 shows the observed and simulated monthly precipitation. This is the same quantity as in the lower left plot of Figure 10, but this time we have plotted each month separately. During the summer month the LOM seems to overestimate quite a lot the monthly precipitation for some of the stations. Such stations are mainly located inland (not shown). The explained variance goes from little above 0.5 for the winter months to around 0.3 in the summer months.

Finally, the simulations aggregated at yearly scale (lower right plot in Figure 10 and Table 1) are quite good, still the quality of the model performance has a clear spatial structure (not shown) with better performances along the coast. Notice how this plot based on LOM predictions at gauge locations gives a much better agreement between LOM and MET annual precipitation than Figure 2, which is based on the same LOM data, but at all locations. Again, this highlights the fact that we lack data to verify LOM at the locations where it predicts the highest precipitation.

3.3 Areal accumulated precipitation

Areal accumulated precipitation is an important component in hydrological modeling. Areal statistics depend on the correlation structure of the data set. In this section we examine how the LOM can reproduce observed statistics of areal accumulated precipitation.

Figure 18 shows the empirical spatial correlation function for the precipitation intensity (i.e. computed only on days with contemporary positive precipitation). The simulated precipitation data set has a stronger correlation structure than the observed one. Many stations with a distance between 200 and 400 km are much more correlated in the simulated data set than in the observed one. At the largest distances, the observed correlation tends to be negative. This is not replicated by the LOM simulated data set where at all distances there is positive correlation. At the shortest distances, on the

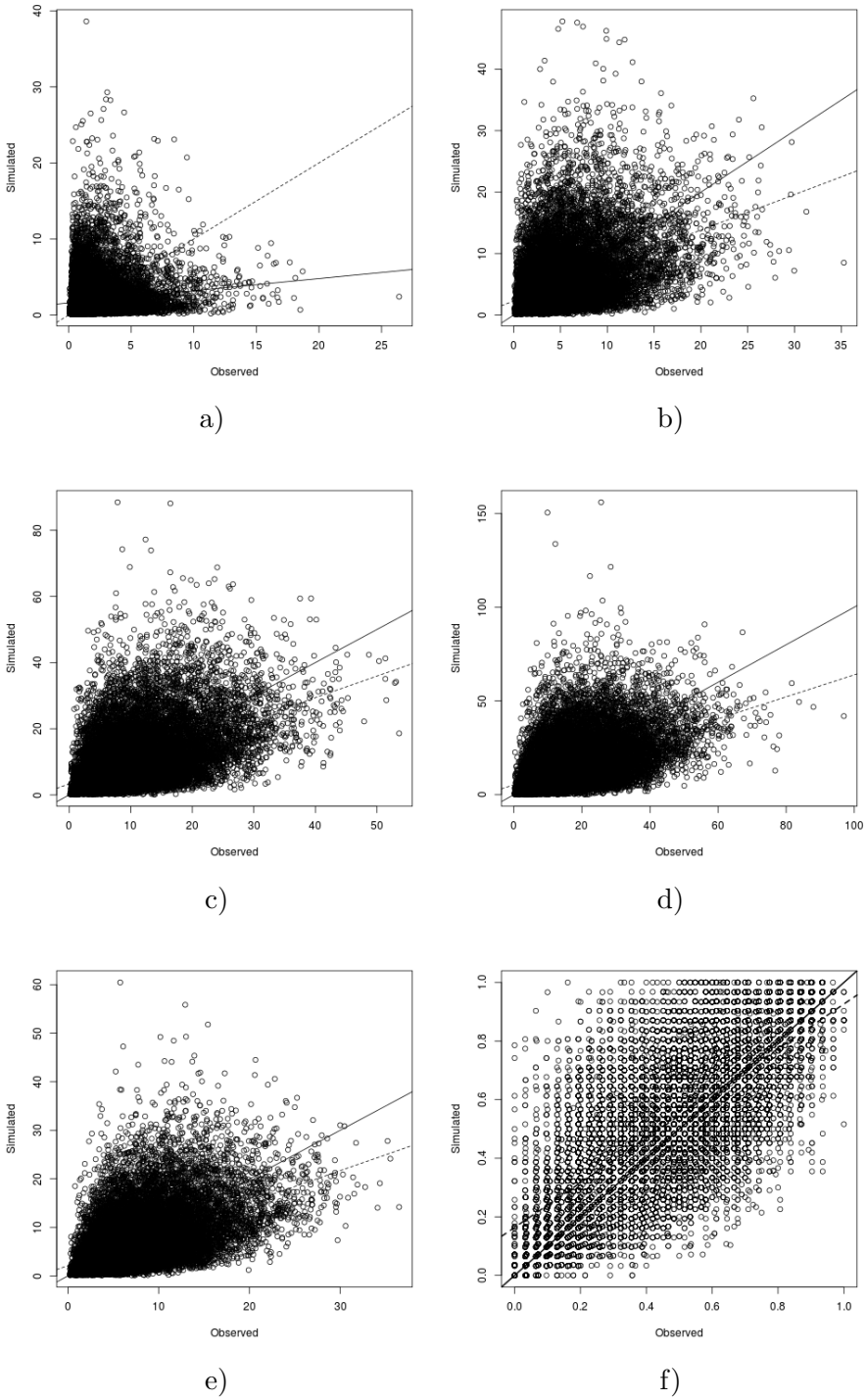

Figure 14: Comparison of statistical characteristics of daily LOM simulations and gauge data calculated each year, for each month over the period 1990-1999. (a)-(d) 25%, 50%, 75% and 90% quantile. (e) mean and (f) probability of no-rain-

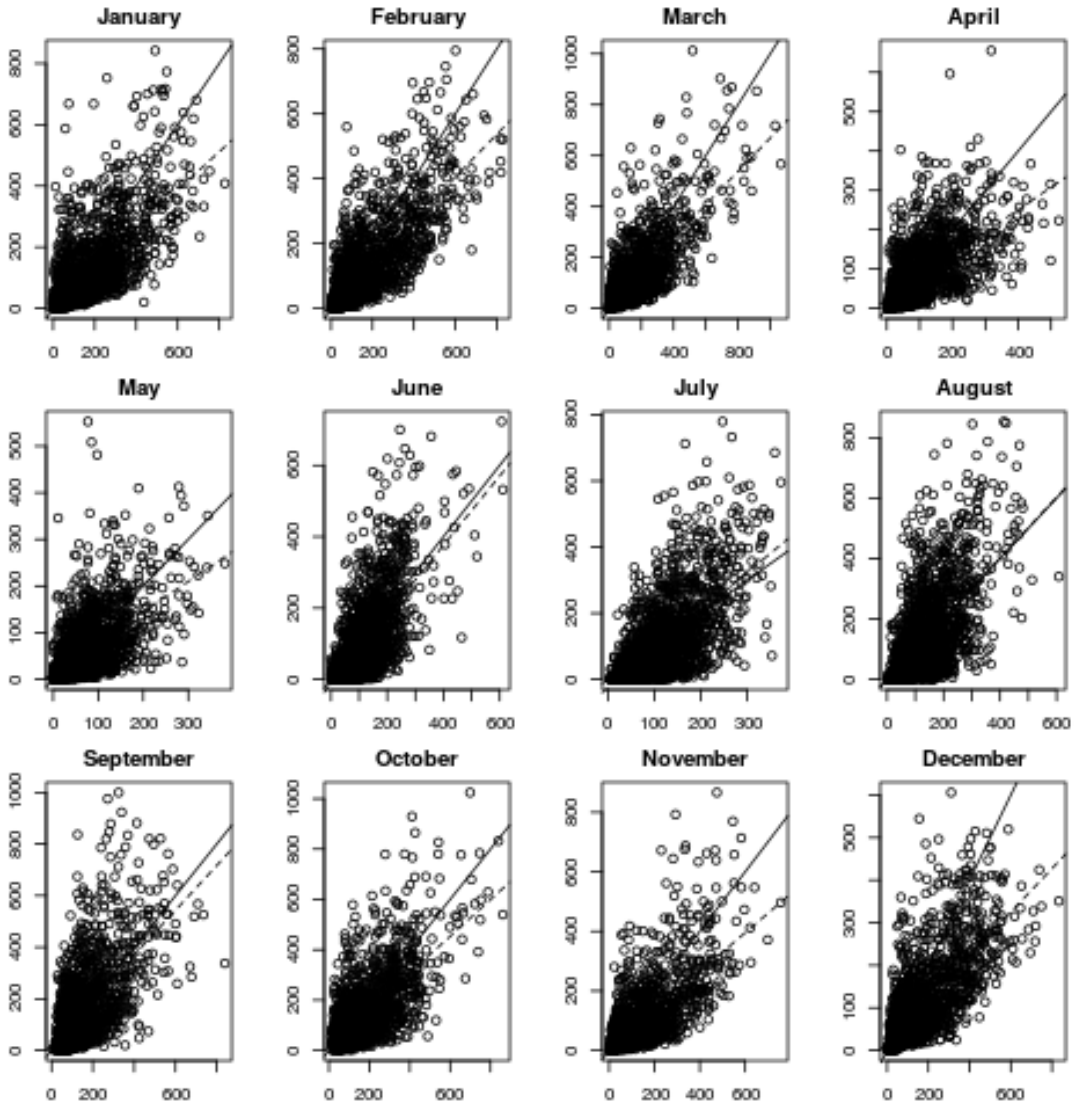

Figure 15: Observed and simulated monthly intensity of precipitation.

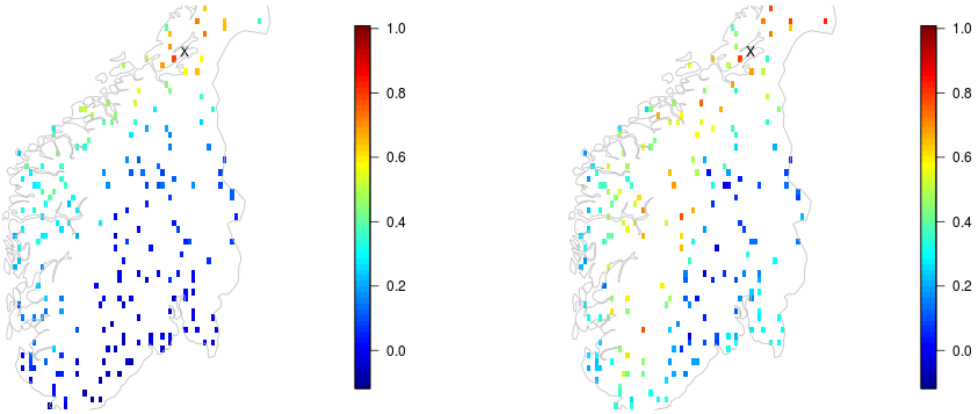

Figure 16: Spatial correlation for the precipitation intensity between station 197 (indicated by a cross) and all the other stations. On the left is the correlation computed in the observed data set, on the right the correlation computed in the simulated data set.

other side, some stations with short geographical distance show lower correlation in the simulated data set than in the observed one.

The larger correlation in the LOM data set is not surprising if we remember that the input of the LOM is spatially averaged, that means that all the stations located in the same sub-domain are subject to exactly the same input. Moreover the LOM only "sees" the orography of the domain and not the distances, so location with the same orography tend to be more correlated than they are in reality. Post-processing the LOM output using a reduced vapor flux as explained in Section 3.1.5 has reduced this phenomenon but it is still quite visible also in the corrected precipitation maps. As an example, Figure 16 shows the estimated correlation between Station 197 (indicated with a cross) and all the other stations in both the observed and the simulated data set. While in the observed data set the correlation drops quite fast with the geographical distance, in the simulated data set there are stations far in the south with a high correlation.

The total number of daily wet stations gives us an idea of how dry each day is over the whole domain. Figure 17 displays the observed frequencies of the number of wet stations together with its simulated counterpart. The largest disagreement between the simulated and the observed quantities is related to the number of days where no rain is recorded in any station. While in the observed data set the percentage of days when all stations are dry is below 1%, in the simulated data set it is above 4%. The LOM also tends to simulate too little days when all the stations (or almost all) are wet.

Finally we check whether the LOM, fed with the ERA Interim parameters, can replicate the observed variability of annual total precipitation averaged over the 9 different

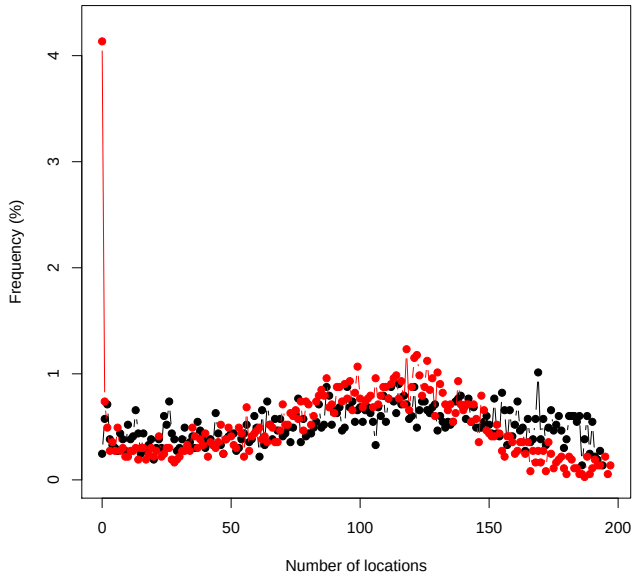

Figure 17: Observed (black) and simulated (red) frequency of total number of stations with positive precipitation.

regions. This region are defined by MET (Hanssen-Bauer et al., 2015) and illustrated in Figure 1b).

To this end, Figure 19 displays observed and simulated annual regional mean precipitation for our 9 precipitation areas plotted against each other. There is a good agreement between the observed and simulated quantities for the areas on the West coast (areas 3,4,5 and 7). Regions 2 (Agder) and 9 (Trndelag) show an additive bias: the LOM underestimates the annual regional mean precipitation but there is a good correspondence between observed and simulated quantities. The two inland areas 1 (Southeast) and 6 (Dovre-Tynset) see a poorer correspondence between observed and simulated regional annual total precipitation, the situation being worse for region 6.

4 Discussion of the Downscaling Experiment

We have used the LOM to construct simulated daily time-series of precipitation over the south of Norway. The input parameters for the LOM are the spatially averaged values of geopotential height, wind, temperature and total precipitation from the ERA-Interim reanalysis data.

We have compared such time series with observed precipitation values from a grid of 197 gauge stations belonging to the Norwegian Meteorological Institute. Such comparison has been done separately for the occurrence process and for the precipitation

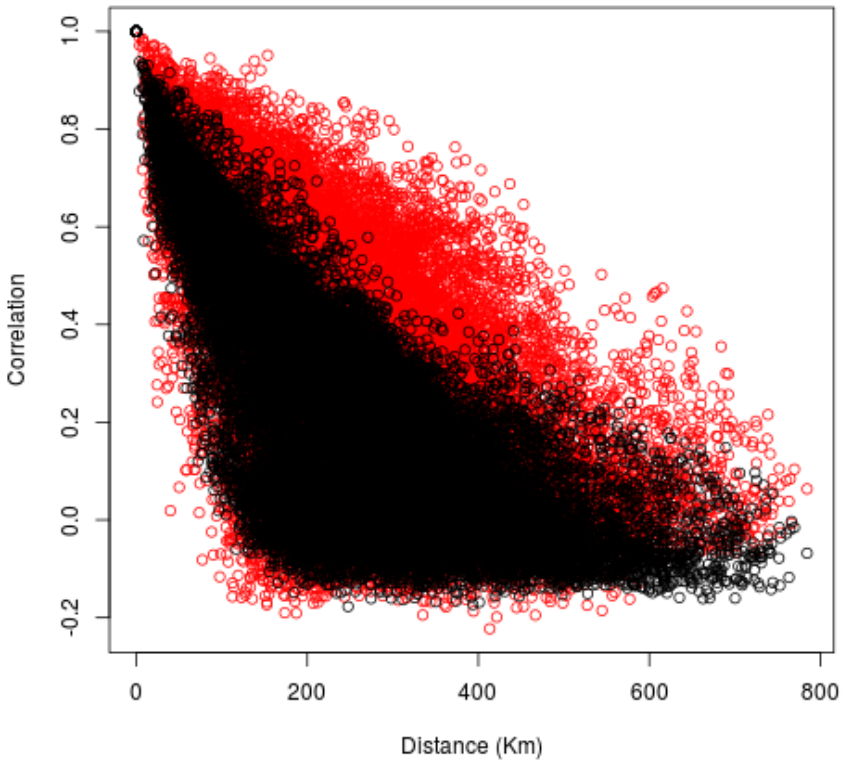

Figure 18: Observed (black) and simulated (red) empirical spatial correlation for daily precipitation intensity.

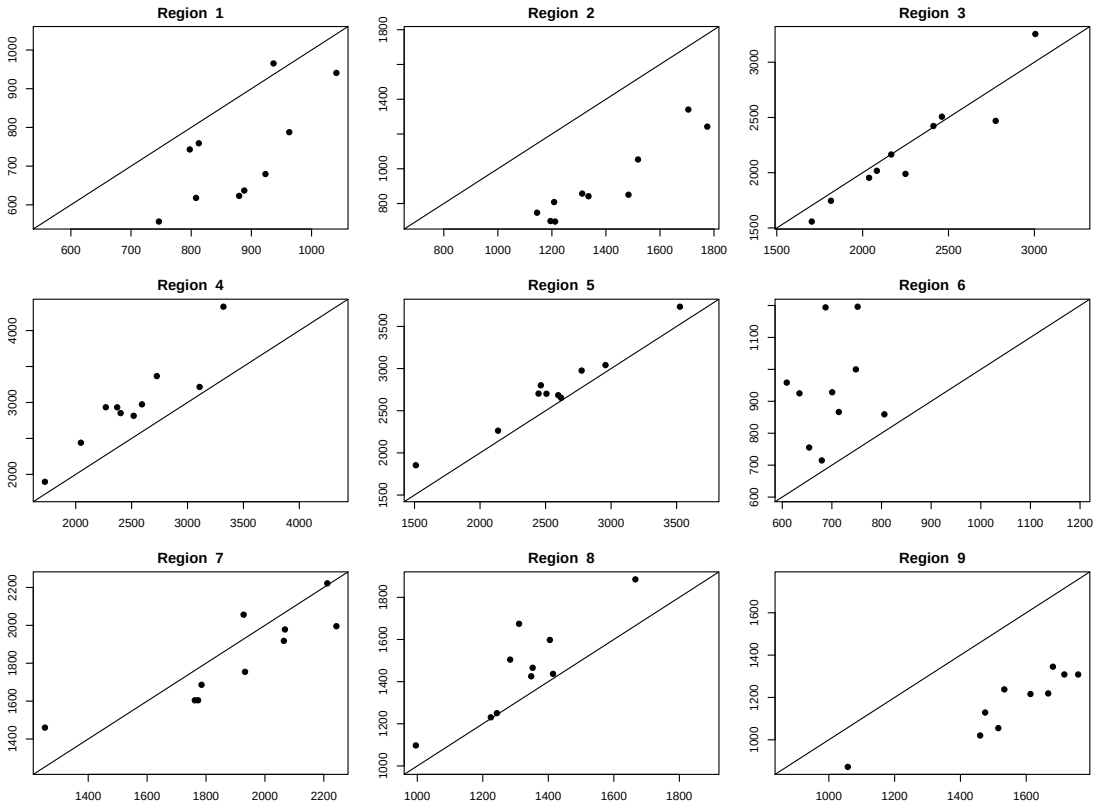

Figure 19: Observed (x-axis) vs Simulated (y-axis) regional annual mean precipitation for the nine areas defined in Figure 1b).

amounts at different aggregation time scales.

It is important to bear in mind that only the domain-average precipitation from ERA-Interim is used in computing the LOM simulations, no information of spatial variability in precipitation is transferred from ERA-Interim to LOM. Moreover, the input atmospheric variables, with the exception of the relative humidity (that is geopotential, temperature, wind and total precipitation) are spatial averages and held constant over the whole domain. Last, the LOM is meant to simulate only one type of precipitation, namely the orographic enhancement of precipitation and does not simulate precipitation coming from other physical processes such, for example, convective precipitation.

Still, the LOM manages to recover quite well many of the spatial characteristics of the precipitation fields in the South of Norway. The simulated yearly maps, present a realistic spatial structure even though they clearly overestimated precipitations in some areas.

There are some bias both in the spatial and in the temporal distribution of the statistics we have taken into account in this study. Not surprisingly, the LOM is much better at recovering the precipitation in the coastal, mountainous regions than inland. The largest discrepancies, both regarding the occurrence and the intensity process, are, in fact, observed in the stations located on the east side of the mountain range.

As for the time dimension, the LOM simulations are closer to the observed data during the autumn and winter season, and a less good predictor during summer. This could be due to the higher proportion of rain due to convective phenomena in summer than in winter. This creates a large small-scale variability which the LOM does not aspire to simulate. Still the LOM appears to overestimate the precipitation during the summer months rather than under-estimate it.

The performance of the LOM when compared to observed data varies with the accumulation period considered. The longer the accumulation period, the better the correspondence between simulated and observed data. This agrees with the findings in Johannesson (2012) where the minimum accumulation period considered is three days. For the daily precipitation the correspondence between simulated and observed data set is very variable both in space and in time. Again, the coastal stations and winter periods are better reproduced by the LOM simulations.

Performance when comparing simulations and observations from day to day ranges from very good to very poor. Surprisingly, it was not possible to define stable criteria for predicting a priori which days would yield good performance and which days would yield poor performance. Moreover, the simulated daily precipitation appears to have a spatial correlation structure with some features that do not appear in the correlation structure estimated from the observed data. Stations that are quite far in space and virtually uncorrelated when looking at the observed data set appear to have a strong spatial correlation in the simulated one. This could be, at least partially, corrected by adding a convection generating mechanism with small spatial range and/or improving the post-processing algorith which computes the air-flow depletion. Often, in days with poor perfomance, the main error lies in the localisation of wet and dry area, the same phenomenon is also reported in Crochet (2007).

In general it appears that the LOM, with the set-up and input choices made in this report, can be a good way to reconstruct climatological precipitation maps (which are based on long accumulation times). The variability of the performance makes it difficult to recommend its use on short time aggregation periods like daily or hourly, where its prediction skill is slightly lower that obtained using the ERA-Interim precipitation maps directly. It is noteworthy, however, that the LOM achieves this skill level for detailed, information-rich precipitation maps, whereas the ERA-Interim predictions are smooth surfaces for which locational errors produce only small residuals. It would be advantageous, therefore, to analyse these results using scale-discriminating techniques, to see if a moderate lowpass filter on the LOM output could reduce the small-scale noise and still preserve most of the intermediate-scale information. This has been outside the scope of the current investigation.

We have chosen to post process the output of the LOM (using a smooth humidity factor and reducing the vapor flux) in order to try to fix some of the know model biases. Possibly better post-processing algorithms could be developed. The introduction of the reduced vapor flux, for example, improved the results with respect to a previous experiment were no post-processing was involved, still the high spatial correlation between stations which are very far but have similar orography shows that, with the current post-processing algorithm, not enough of the water vapor flux is depleted downwind once the airflow has passed over several hills.

The gauge data are not corrected for wind induced undercatch. The reason for this is that wind is generally not measured at the station sites, leaving fixed exposure compensation as the only option. An exposure classification does exist (Førland et al., 1996), but has large uncertainties in addition to no temporal variability. The two most obvious expected effects of not correcting gauge data before evaluating the LOM, would be 1) an apparent general LOM over-estimation of precipitation, and 2) stronger apparent over-estimation during winter than during summer. As revealed by figures 10 and 15, the opposite result is evident for both of these.

To end, the LOM is quite easily implemented and run on a PC, and the simulations are very fast. The model set-up and parametrization, on the other side, are not trivial. Many choices have to be taken with respect to the physical variables that are involved in the computations, for instance the atmospheric pressure levels from which to calculate gradients and the Brunt-Vaisala frequency, the hydrometeor formation time etc). It is possible that the strong physical basis makes the LOM too sensitive to data with large uncertainty. Influential is also the size of the spatial domain, since the LOM assumes nearly all input to be spatially homogeneous. The sub-domains used in this investigation were defined on the basis of the MET definition of precipitation areas in Norway. Other choices could have been possible.

5 Enki implementation

In addition to the R implementation, the orographic model is implemented in C++, both as a self-standing library callable from e.g. Python as well as other C++ programs, and

as an extension to the two standard Enki interpolation routines (Kriging and IDW). It will also work under IDW's two special cases (all-map average and nearest-neighbor interpolation). The extension of LOM to apply a downstream depletion of moisture (3.1.5) is included in the Enki implementation, but the humidity correction (3.1.4) is not.

The Enki implementation is primarily directed towards using LOM as a part of daily operational simulation, unlike the original stochastic weather generator context. The LOM process representation itself is not affected by this, but these routines post-process the LOM output together with the precipitation input data. In addition to some diagnostic variables, two main output variables are produced:

1. The raw, simulated output from LOM
2. The interpolated precipitation surface using LOM as an external trend.

In short, the first of these forms a gridded map of pure LOM output. From this surface, LOM values at gauge locations are extracted, and the differences between these and the original observations are noted. These differences are now interpolated to a new gridded surface, which is added to the LOM output to yield the second output; the final LOM-gauge-combined precipitation map.

In order to allow simulation with minimal input, the primary LOM input characterizing an atmospheric depth profile is reduced to standard ground-based input variables. Depth-average relative humidity is simply replaced with surface values. The temperature lapse rate is estimated from the elevation dependency of surface temperature observations at different altitudes, which is clearly a non-optimal estimator for the free-atmosphere lapse rate. Also, as an alternative to accepting wind vectors as input variables, the routines offer the possibility to optimize a synthetic wind vector, selecting from a library the speed and direction which produce the best correspondence between raw LOM output and the station values.

The LOM extensions to the Kriging and IDW methods retain these routines' possibility to perform evaluation by cross-validation. The Enki operator turns on this mode by defining the target geometry (usually the model grid) as identical to the source geometry (the station map). This apparently meaningless interpolation setup is used as a flag to exclude each target location's nearest gauge (which is itself when only gauge locations are considered) from its list of neighbors. It is thus ignored during interpolation, which is the core of the cross-validation technique.

5.1 Evaluation

In addition to the direct comparisons, LOM has been evaluated as a trend surface generator to support spatial interpolation of precipitation. As a predictor of how the terrain influences precipitation, LOM output can be seen as an alternative to the elevation lapse rate. This experiment was performed using the Enki implementation of the LOM.

The case study selected is a 26000 km^2 mountainous area in Norway (Fig. 20), around the main water divide. Elevations range from 0 to 2469 m a.s.l. Annual precipitation

varies from below 500 mm to more than 2000 mm. Data are daily observations from 60 stations, with standard correction for wind-driven undercatch.

Interpolation with LOM support was evaluated using the leave-one-out cross-validation method. A station is withheld from interpolation, and compared to the value estimated at its location. The exercise is repeated for all stations, over time generating a space-time array of differences. This array can be summarized along both rows and columns, corresponding to spatial and temporal performance at each day or each station, respectively.

For absolute characterization of performance, a weakness of the method is that the exclusion of stations alters the distribution of neighbor distances, so the station network analysed appears sparser than the true network. Comparing different methods in the similar way, this effect largely cancels out. For spatial and temporal comparison, the temporal and spatial vector of results, respectively, were condensed into a single average NSE (Nash-Sutcliffe Efficiency Criterion). It may be noted that this measure, by normalising w.r.t variance, give very poor values on nearly-dry days.

5.2 Results

A somewhat surprising experience from the initial analyses is that the estimation of covariance structure (Semivariogram) used for the interpolation, showed that the most of the variability in this station network takes place at scales below the station density. This resulted in very high nugget estimates, suggesting that around 70% of the variance is small-scale 'noise' (variance at non-detectable scales). It is possible to force a low nugget value (for instance, see it as an observation variance), but this simply results in covariance ranges being estimated to less than five km. As an evaluation of the LOM per se, this data set is thus not optimal.

In the main experiment, three different interpolation techniques (Kriging, Inverse Distance, and simple average) were calibrated and combined with four treatments of terrain-dependent correction (None, gradient (-H), LOM with ERA wind (-EW), and LOM with optimised wind (-OW)). Bar diagrams showing the cross-validation performance are shown in Fig. 21 for temporal performance, and Fig. 22 for spatial performance.

It is striking that spatial NSE tend to be on average negative, whereas temporal NSE achieves moderate values around 0.35. Using correlation rather than NSE give around 0.08 and 0.6, indicating that bias plays a considerable role in the low NSE values. The low spatial correspondence appears because the region-wide synchronous response to overall dry days or large frontal situation is not influencing spatial NSE (or correlation). Also notable is that the interpolation method seems more important than the terrain correction, and that a crude spatial mean performs better than IDW.

5.3 Elevation gradient versus Linear Orography Model

In figures 21 and 22, Kriging and IDW respond differently to the two terrain-driven corrections, with IDW seemingly preferring elevation gradient, whereas Kriging favours

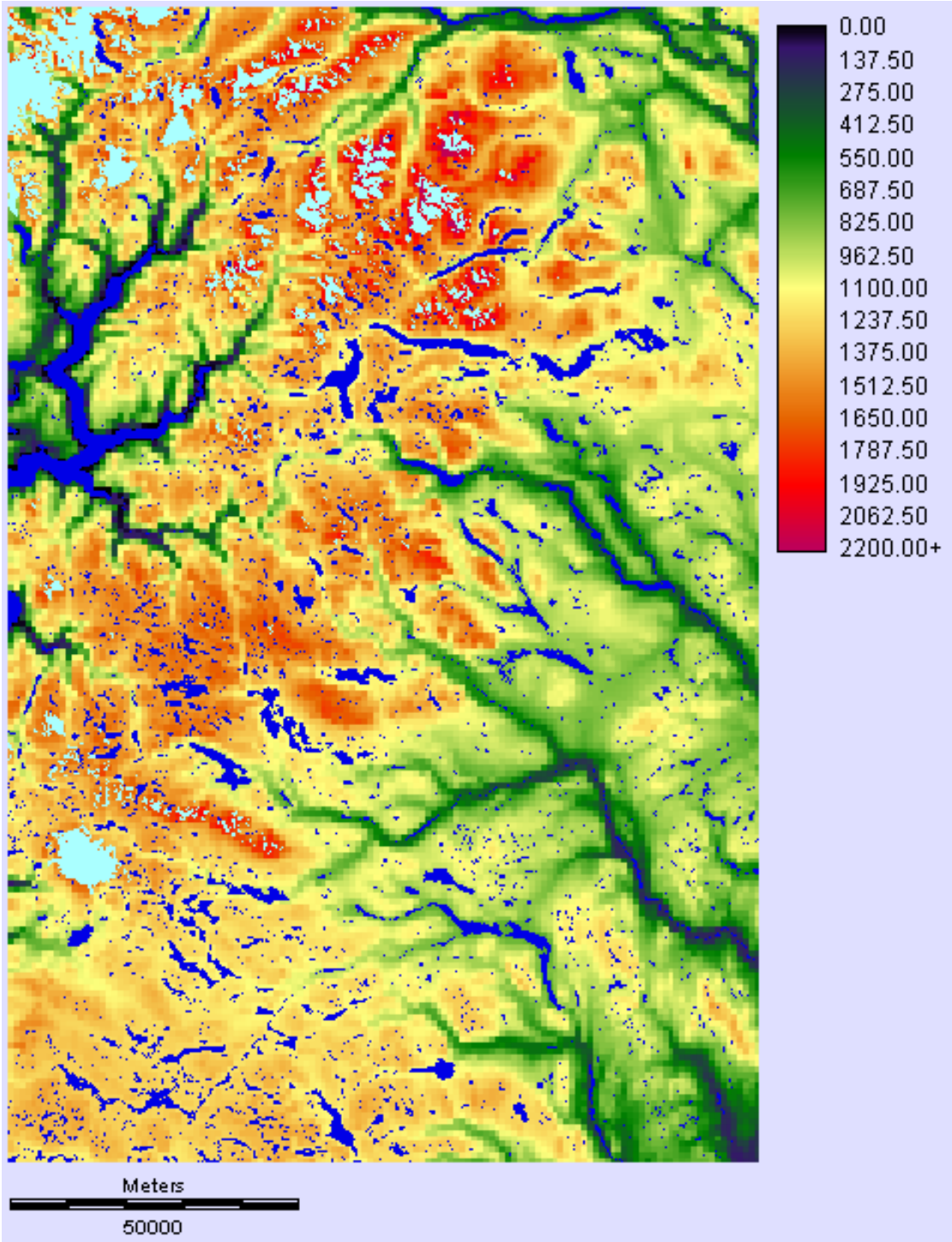

Figure 20: Elevation map over the study area used for evaluating the LOM in precipitation interpolation

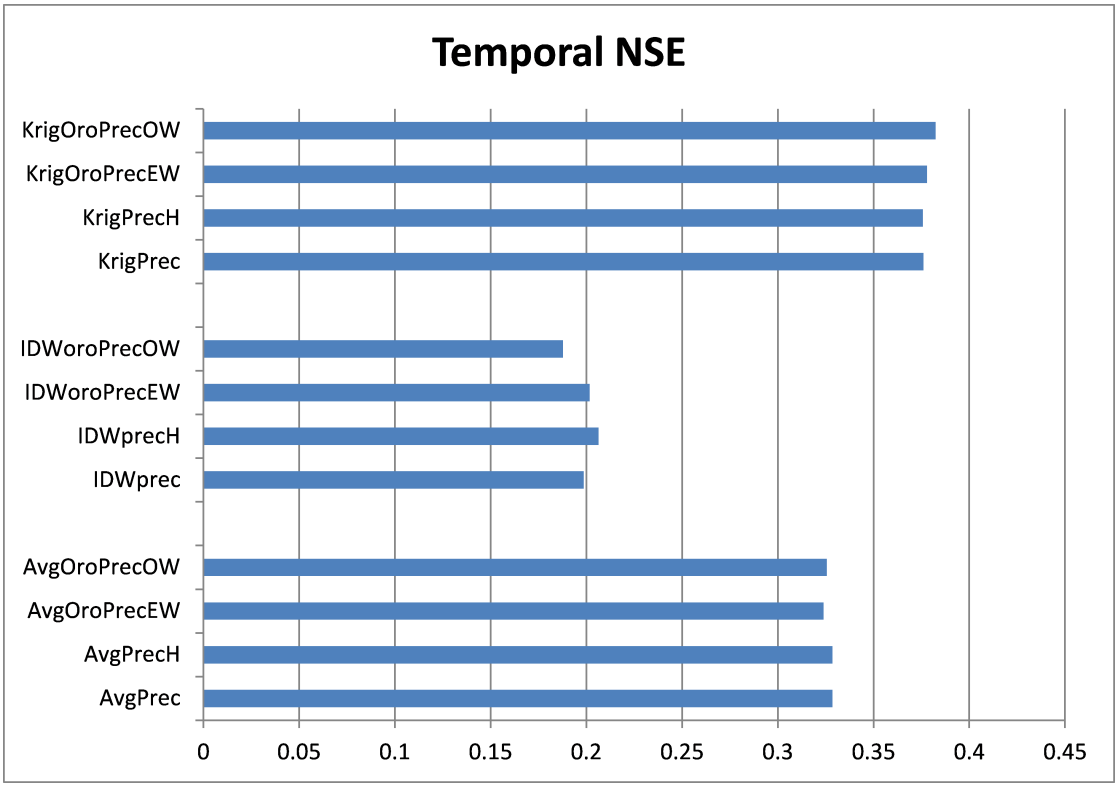

Figure 21: Temporal NSE from cross-validation

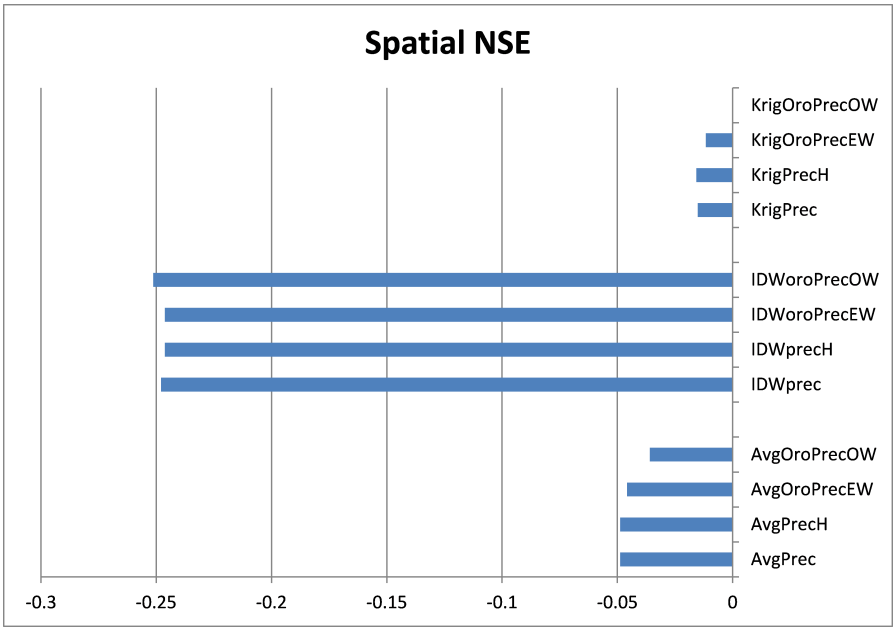

Figure 22: Spatial NSE from cross-validationp

LOM. The overall effect of both corrections, however, is small when compared to the overall variance. This may be partly connected to the NSE expressing the ratio of explained to total variance, and that LOM is only being run for a subset of days. The distribution of variance and interpolation performance on days with or without LOM being operated, have not been compared. Avoiding variance normalised measures, we can look at the number of cases where the gradient or LOM improves the performance. This view favours LOM versus the elevation gradient, as can be seen from table 2 showing the number of days on which the corrections improve the estimates.

It is clear that with the atmospheric temperature and moisture profiles estimated

Elevation	Days inapplicable or with no effect:	Fraction of days with improved performance	Fraction of days with poorer performance
Elevation gradient	2%	39 % (max NSE 0.056)	59 % (min NSE -0.052)
LOM, ERA Interim wind	84 %	12 % (max NSE 0.200)	4 % (min NSE -0.002)
LOM, optimised wind	64 %	29 % (max NSE 0.230)	7 % (max NSE -0.065)

Table 2: Number of days on which the corrections improve the estimates

from ground stations only, a large majority of days are classified as not satisfying LOM operating conditions. Selecting the best synthetic wind vector to some extent improves the situation. Negative results may still occur because the library of standard wind vectors is pre-produced using LOM-favourable temperature and humidity conditions, whereas the actual estimation is based on measured temperature. At last, it must be remembered that none of the current evaluations of the linear orography model compare it to measurements of what the model actually predicts. Neither do the attempts to account for stratiform precipitation fully remove its influence; and the total lack of convective processes is even more obscuring the results, in particular for variance-based measures. The main LOM process representation, and in particular its improvement from the pure upslope model, mainly address spatial variance in a small scale where gauge based evaluation (using the standard national network) does not bring sufficient data to the evaluation.

6 Conclusion and recommendations

- Comparing LOM simulations at gauge locations with gauge observations, the LOM is reasonably well performing in terms of overall bias, with a slight underestimation of average values. The LOM volumes are not calibrated, and the observations are not corrected for catch deficit. The variance is also underestimated in the LOM output, more for daily aggregation than for weekly, monthly and annual aggregation.

- Visually comparing gridded LOM maps at 1km resolution to 1km interpolated maps from MET, the LOM predicts much larger spatial variability than MET's interpolated precipitations maps. This is due to 1) a dominance of locations with smoothed values on the interpolated map, and 2) a tendency for LOM output to be very high in some high-altitude and glaciated areas, which are generally ungauged.

- The spatial correlation between LOM predictions and gauge recordings is good for annual and monthly aggregation, but poor for daily data. This makes LOM a good alternative to i.e. an elevation lapse rate for climatology, but indistinguishable for short time scales. It is believed that a major reason for this is uncertainty in LOM's input data forcing and unrealistic assumptions of homogeneity, to some extent supported by the improvements obtained by trying to mitigate these by post-processing LOM predictions.

- The correspondence between LOM and gauge data is good at large scales, both spatial and temporal, for instance by correctly locating a high-precipitation zone well to the west of the mountain range, rather than along the main water divide.

- The spatial correspondence is poorly documented at small scale due to a sparse network of precipitation gauges. Important small-scale processes simulated in the LOM are therefore left largely non-validated.

- The correspondence between LOM output and gauge data is better along the coast, in particular in Western Norway, than in the Eastern inland areas.
- The correspondence between LOM output and gauge data is better during winter, spring and autumn than in the summer.
- The LOM, as driven by ERA-Interim forcing, slightly over-estimates the probability of dry days, mainly due to a bias during the summer months. The main spatial pattern in the P_0 probability is recreated.
- For two consecutive days, the dry to wet (zero to non-zero precipitation) transition probability is underestimated, (and the dry to dry probability is correspondingly overestimated) by the LOM as compared to gauge data.
- The mean duration of wet spells (number of consecutive days with precipitation) is well simulated, whereas the mean dry spell length is markedly over-estimated, in particular in South-Eastern Norway.
- The temporal variability in LOM performance is high; some days the spatial pattern is excellently predicted, some days LOM fails completely. The project has not succeeded in modelling this variability by explanatory variables.
- The spatial correlation structure for daily data is in general stronger in LOM predictions for gauge locations than in the gauge data themselves. This is due to the input-homogeneity assumption, and that some stations are very similarly situated in terms of topography, but far apart in distance.

6.1 Recommendations

As a general model for topographic influence on precipitation, the LOM predicts well the main features of climatological precipitation distribution in southern Norway. It correctly locates the highest precipitation between the Western coast and the main water divide, and not along this divide itself, as would the more commonly used lapse rate. The LOM predicts some very high values in locations without measurements, and in practical use, one may want to filter out the most extreme predictions. Explaining 53% of the spatial variance in annual precipitation, however, the LOM can be recommended as a clear improvement from the lapse rate as a correction of spatial precipitation bias.

An important purpose of the LOM is to predict small-scale spatial variability. Several terms in the model (air flow dynamics, formation and fallout time scales) represent processes which have their main consequences at scales below 20 km. This is below the typical gaugedensity, and these properties of the LOM output have been difficult to evaluate by the gauge data in this investigation. The cross-validation evaluation reveals a very high short-distance variance (nugget) in the gauged data, but also that LOM adds little skill to the interpolation, i.e. explains little of this short-distance variance. This investigation therefore does not lead to a recommendation of the LOM for downcaling in the range below 30 km.

For the purpose of the Stochastic Weather Generator project under which this investigation has taken place, explicit downscaling by the LOM is currently replaced by empirical transfer models tuned at the station level, but with parameters interpolated to complete maps. This means that topographic effects are represented to the extent that they are evident in the recorded values, whereas the small-scale variability governed by terrain data alone is abandoned. This may change as research progresses.

6.2 Further work

It is our belief that simple models of orographic enhancement could be more fruitful for practical application than we have been able to prove in his project. This includes application for shorter temporal and spatial scales.

An obvious line of continued research into using the LOM for downscaling precipitation, is to improve its forcing. This may include using a larger set of values from the ERA-I columns, replacing ERA-I with real radiosonde measurements, and decreasing the domain size to make the homogeneity assumption more realistic. Indications that such attempts may lead to improvement are found in the positive effects of adding downwind depletion and humidity scaling.

Another line is to improve the evaluation technique, in particular by investigating more directly the scale decomposition of the difference between two spatial images. This could help understanding the reasons behind the well- and poor-performing aspects of the LOM, and provide guidelines for modifying the model itself or its pre/post processing routines. Support for this were found in a comparison between LOM-generated daily maps and the spatially variable ERA-I precipitation estimates. The latter were of course very smooth compared to the LOM maps, which is usually favoured in comparisons. Still the two showed comparable skill in predicting gauge values.

This investigation has revealed that gauge data from the national daily network is insufficient to evaluate all aspects of the LOM simulations, in particular the small-scale effects of air flow dynamics and formation/fallout time scales. A next step could be the use of weather radar data, which in addition to high detail level would also limit the uncertainty in input data and provide much better diagnostics. Also, runoff recordings and satellite-derived SWE maps (Kolberg and Gottschalk, 2010) could enrich the validation data set.

It should be noted that both a two-layer LOM version (Barstad and Shuller, 2011) and a considerably more detailed simulator ICAR (Gutmann et al., 2016) for downscaling precipitation have been proposed, suggesting the direction for improving the results by adding more precise process description.

For free simulation, it could be beneficial to add a separate large-scale precipitation generator and a convection generator, and to calibrate/evaluate the sum of these three jointly, rather than comparing the single-process LOM against precipitation resulting from several processes. This is particularly linked to the LOM's poor handling of instability in the atmospheric column.

References

Barstad, I. and Shuller, F. (2011). An extension of smiths linear theory of orographic precipitation: Introduction of vertical layers. *Journal of Atmospheric Science*, 68:2695–2708.

Barstad, I. and Smith, R. B. (2005). Evaluation of an orographic precipitation model. *Journal of Hydrometeor*, 6:85–99.

Crochet, P. e. a. (2007). Estimating the spatial distribution of precipitation in iceland using a linear orographic precipitation. *Journal of Hydrometeor*, 8:1285–1306.

Førland, E. J., Allerup, P., Dahlström, B., Elomaa, E., Jonsson, T., Madsen, H., Perälä, J., Rissanen, P., Vedin, H., , and Vejen, F. (1996). *Manual for operational correction of nordic precipitation data*. Norwegian Meteorological Institute.

Gutmann, E., Barstad, I., Clark, M., Arnold, J., and Rasmussen, R. (2016). The intermediate complexity atmospheric research model (icar). *Journal of Hydrometeorology*, 17(3):957973.

Hanssen-Bauer, I., Frland, E. J., Haddeland, I., Hisdal, H., Mayer, S., Nesje, A., Nilsen, J. E. ., Sandven, S., Sand, A. B., A., S., and dlandsvik B. (2015). Klima i norge 2100. kunnskapgrunnlag for klimatilpassing oppdatert 2015. NCCS report 2/2015, Milidirektoratet.

Johannesson, T. e. a. (2007). Effect of climate change oh hydrology and hydro-resources in iceland. Technical Report Report OS-2007/011, Reykiavik: National Energy Authority.

Johannesson, T. e. a. (2012). High resolution precipitation mapping in iceland by dynamical downscaling of era-40 with a linear orographic precipitation. Technical Report Report 2012-003, Icelandic Meteorological Office.

Kolberg, S. and Gottschalk, L. (2010). Inter-annual stability of grid cell snow depletion curves as estimated from modis images. *Water Resources Research*.

Sinclair, M. R. (1994). A diagnostic model for estimating orographic precipitation. *Journal of Applied Metereology*, 33:1163–1175.

Smith, R. B. and Barstad, I. (2004). A linear theory of orographic precipitation. *Journal of Atmospheric Science*, 61:1377–1391.

Smith, R. B. and Evans, J. P. (2007). Orographic precipitation and water vapor fraction over the southern andes. *Journal of Hydrometeorology*, 8:3–19.